Available online at www.sciencedirect.com
ScienceDirect
Comput. Methods Appl. Mech. Engrg. 315 (2017) 1025–1052
Computer methods in applied mechanics and engineering
www.elsevier.com/locate/cma

A multisymplectic integrator for elastodynamic frictionless impact problems

François Demoures[a,b], François Gay-Balmaz[b,*], Mathieu Desbrun[c], Tudor S. Ratiu[d,e], Alejandro M. Aragón[f]

[a] *Department of Mathematics, Imperial College, London, United Kingdom*
[b] *CNRS-LMD-IPSL, École Normale Supérieure de Paris/CNRS, Paris, France*
[c] *Computing +Mathematical Sciences, Caltech, 1200 E. California Blvd, Pasadena, CA 91125, USA*
[d] *School of Mathematics, Shanghai Jiao Tong University, Minhang District, Shanghai, 200240, China*
[e] *Section de Mathématiques, École Polytechnique Fédérale de Lausanne, CH–1015 Lausanne, Switzerland*
[f] *Department of Precision and Microsystems Engineering, Faculty of 3ME, Delft University of Technology, Mekelweg 2, 2628 CD, Delft, Netherlands*

Received 6 October 2015; received in revised form 1 November 2016; accepted 2 November 2016
Available online 8 December 2016

Abstract

We present a structure preserving numerical algorithm for the collision of elastic bodies. Our integrator is derived from a discrete version of the field-theoretic (multisymplectic) variational description of nonsmooth Lagrangian continuum mechanics, combined with generalized Lagrange multipliers to handle inequality constraints. We test the resulting explicit integrator for the longitudinal impact of two elastic linear bar models, and for the collision of a nonlinear geometrically exact beam model with a rigid plane. Numerical simulations for various physical parameters are presented to illustrate the behavior and performance of our approach.

Keywords: Structure preserving discretization; Collisions; Elastic bodies; Multisymplectic integrator

1. Introduction

The accurate modeling of impacts between elastic materials is one of the main difficulties in a variety of engineering applications. Consequently, the design of numerical methods addressing impact problems has been an important endeavor in mechanical engineering, computational science, and even computer animation. In contrast to smooth mechanics, contact problems must deal with the singularities that collisions induce. Numerically handling these discontinuities, in a manner that respects the inequality conditions and conserved quantities that are expected from the dynamics, has been an important scientific challenge. To this day, no solutions satisfying both physical expectations and computational constraints exist. Radically new approaches are most certainly necessary to successfully address these issues.

* Corresponding author.
E-mail addresses: demoures@lmd.ens.fr (F. Demoures), francois.gay-balmaz@lmd.ens.fr (F. Gay-Balmaz), mathieu@cms.caltech.edu (M. Desbrun), ratiu@sjtu.edu.cn, tudor.ratiu@epfl.ch (T.S. Ratiu), A.M.Aragon@tudelft.nl (A.M. Aragón).

http://dx.doi.org/10.1016/j.cma.2016.11.011
0045-7825/

Our novel approach for the numerical treatment of collisions is motivated by the belief that the field theoretic (or multisymplectic) point of view, traditionally adopted in geometric mechanics, can be key to the development of variational integrators for PDEs involving contact. We propose a proper discretization of nonsmooth multisymplectic variational mechanics to circumvent the numerical issues that have plagued previous methods. In particular, we take advantage of recent algorithms [1–3] that have already made progress in this direction.

Relevant background

Nonsmooth mechanics has a long history, beginning with the works of Johann (1710), Bernoulli, (1724) Euler (1752), and Fourier (1798); see the excellent narrative of Curnier [4]. The modern treatment of describing the motion of a body in the presence of unilateral contact (see [5] for a concise exposition) has been largely based on the work of Moreau and Rockafellar in nonsmooth convex analysis [6–10]. The resulting computational contributions to contact mechanics include [1,11–20]; see [21] for an account of the differences between these various methods.

Discrete variational mechanics has its roots in the optimal control literature of the 1960s and in the discrete Lagrangian formalism from [22–24], which fits nicely within the variational framework. The variational view of discrete mechanics and its numerical implementation have been developed in the past decade, see, e.g., [25–30]. The extension of this discrete variational framework to continuum mechanics has been carried out in [31] by means of multisymplectic variational integrators. We refer to [3,32] for the development of multisymplectic integrators on Lie groups and its application to geometrically exact beams. Variational integrators for fluid dynamics have been developed and applied to several fluid models in [33–35].

Contributions

In this paper, we introduce a field theoretic integrator for elastodynamic and frictionless impact problems that combines a multisymplectic (spacetime) variational approach [36] with optimization techniques to minimize the action functional over impenetrability constraints ([5,37]). Collisions are numerically handled via a generalized Lagrange multiplier approach for constrained optimization problems as formulated in [37]; we do not consider penalty methods or the theory of augmented Lagrangians in this work. Based on the recent theoretical results in [21], we develop a fully space–time variational formulation of both the continuous and discrete settings, thus advancing further the vision originally outlined in [36]:

> "*Perhaps the most important task is to develop algorithms and a discrete mechanics for nonsmooth multisymplectic variational mechanics and to take advantage of the current algorithms (such as that of Pandolfi, Kane, Marsden, Ortiz* [1]*) that are already developing in this direction*".

Scope

We illustrate our contributions through two examples. We first simulate the longitudinal impact of two one-dimensional elastic bars, a classical benchmark in the literature [12,18,38,39]. We show that we can obtain prolonged contact without ad hoc treatment of the release time. We then demonstrate our approach on a three-dimensional geometrically exact nonlinear beam model (based on [40]) colliding with a rigid plate, where the initial conditions are given by the configuration and the initial speed of the beam. Displacements of the non-linear beam in time are computed through a multisymplectic Lie group variational integrator [3], and the contact problem is formulated variationally through the introduction of a gap function. Both examples take full advantage of conservation laws of the system.

Outline

In Section 2, we recall the multisymplectic description of nonsmooth continuum mechanics. We derive in Section 3 a variational integrator for nonsmooth continuum mechanics. We illustrate our resulting time stepping algorithm in Section 4 through the simulation of a longitudinal impact of two hyperelastic linear bar models. Two algorithms associated to different discretizations of the bars, and their associated results for different physical parameters, are presented. Then we consider in Section 5 the impact of a geometrically exact nonlinear beam model with a fixed planar obstacle. We test the integrator by considering different speeds of impact, various element sizes Δs of the mesh, and different time steps Δt.

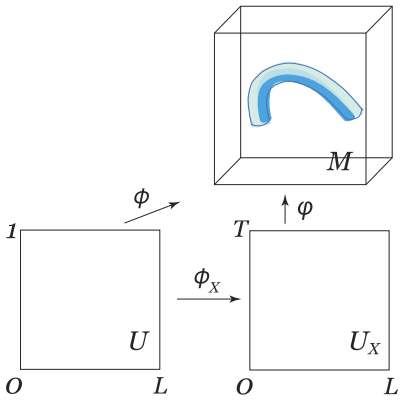

Fig. 2.1. Domains U, U_X, and M, along with the maps ϕ_X, ϕ and φ for 1D + time problems.

2. Field theoretic description of nonsmooth continuum mechanics

In this section, we introduce the field theoretic description of contact problems between two elastic objects. Two examples are used throughout the exposition to illustrate this framework: two elastic beams colliding, and a geometrically exact beam colliding with a fixed plane.

2.1. Field theoretic description in the smooth case

We begin with a review of the main objects that are involved in the field theoretic description of continuum mechanics in the smooth case. The configuration of an elastic body is specified by a map ϕ defined over a domain U that is a subset of spacetime X, with values into an embedding space M. Thus, the configuration field is formally defined as:

$$\phi : U \subset X \to X \times M.$$

The spacetime X. Spacetime is of the form $X = \mathbb{R} \times \mathcal{B} \ni (t, s)$, where $\mathbb{R}$ corresponds to the time component and $\mathcal{B}$ is the *reference configuration* of the elastic body. In this paper, we limit our study to 1D + time problems, so $\mathcal{B}$ is chosen to be a compact interval of $\mathbb{R}$.

The spacetime domain U. The spacetime domain is a compact subset of X, usually of the form $U = [0, 1] \times \mathcal{B}$. It is often useful to consider more general subsets U in order to formulate conservation laws such as Noether's theorem or the balance of configurational forces. For the first example involving two beams of lengths L_A and L_B, we let $U = [0, 1] \times ([0, L_A] \sqcup [0, L_B])$. For the second example with a single beam of length L, $U = [0, 1] \times [0, L]$ instead.

The space M of *current configurations* encodes the degrees of freedom needed to describe the embedding of the body at each spacetime point. From the field theoretic point of view, it corresponds to the fiber of a trivial fiber bundle $X \times M \ni (t, s, m) \mapsto (t, s) \in X$ over spacetime. For a one-dimensional elastic beam, the space M is thus the real line $\mathbb{R}$, see Fig. 4.1. For a geometrically exact beam, the space M is the special Euclidean group $SE(3)$, see Fig. 5.1.

The configuration field ϕ. The *configuration field* $\phi : U \to X \times M$ is a smooth map whose two components are denoted by

$$\phi(\tau, \varsigma) = (\phi_X(\tau, \varsigma), \varphi(\phi_X(\tau, \varsigma))) =: ((t, s), m) \in X \times M. \tag{2.1}$$

The first component

$$\phi_X : U \to U_X := \phi_X(U), \quad \text{with} \quad \phi_X(\tau, \varsigma) = (t, s), \tag{2.2}$$

is assumed to be a smooth embedding of U into X. The map ϕ_X is called the *base space configuration* and encodes all possible reparameterizations of the spacetime domain U; it plays a crucial role in the discrete setting, see Fig. 2.1 and Fig. 3.1. The variations $\delta\phi_X$ of ϕ_X are called *horizontal variations*.

The second component $\varphi : \phi_X(U) \to M$ is a smooth map that describes the *deformation* of the elastic body. It is interpreted as a section of the trivial fiber bundle $U \times M \to U$. Its variations $\delta\varphi$ are called *vertical variations.*

In the example of the contact between the two beams we write

$$\phi : U \to U \times \mathbb{R} \times \mathbb{R}, \quad ((\tau, \varsigma_1), (\tau, \varsigma_2)) \mapsto \big((t, s_1), (t, s_2), \varphi_1(t, s_1), \varphi_2(t, s_2)\big),$$

with $(t, s_i) = \phi_X(\tau, \varsigma_i)$, $i = 1, 2$, and where we recall that $U = [0, 1] \times ([0, L_A] \sqcup [0, L_B])$. Thus $M = \mathbb{R} \times \mathbb{R}$ in this case. For the contact of a beam with a fixed plane, we have

$$\phi : U \to U \times SE(3), \quad (\tau, \varsigma) \mapsto \big(t, s, \varphi(t, s)\big)$$

with $(t, s) = \phi_X(\tau, \varsigma)$ and $U = [0, 1] \times [0, L]$. Thus $M = SE(3)$ in this case.

Euler–Lagrange field equations, balance of energy and configurational forces. The Lagrangian density associated to a 1D + time problem is of the form

$$\mathcal{L}(t, s, \varphi, \partial_t\varphi, \partial_s\varphi) = L(t, s, \varphi, \partial_t\varphi, \partial_s\varphi)dt \wedge ds. \tag{2.3}$$

The associated action functional is defined on a configuration field ϕ by

$$\mathfrak{S}(\phi) := \int_{\phi_X(U)} \mathcal{L}(t, s, \partial_t\varphi, \partial_s\varphi), \tag{2.4}$$

where φ and ϕ_X are given as in (2.1). Stationarity of the action $\mathfrak{S}$ with respect to variations $\delta\varphi$ (vertical variations) yields the *Euler–Lagrange field equations*

$$\frac{\partial}{\partial t}\frac{\partial \mathcal{L}}{\partial \dot{\varphi}} + \frac{\partial}{\partial s}\frac{\partial \mathcal{L}}{\partial \varphi'} - \frac{\partial \mathcal{L}}{\partial \varphi} = 0, \tag{2.5}$$

where, from now on, we use the notation $\dot{\varphi} := \partial_t\varphi$, $\varphi' := \partial_s\varphi$. Stationarity of the action $\mathfrak{S}$ with respect to variations $\delta\phi_X$ (horizontal variations) yields both the *balance of energy* and the *balance of configurational forces*:

$$\begin{aligned} &\frac{\partial L}{\partial t} + \frac{\partial}{\partial t}\left(\frac{\partial L}{\partial \dot{\varphi}}\dot{\varphi}\right) + \frac{\partial}{\partial s}\left(\frac{\partial L}{\partial \varphi'}\dot{\varphi}\right) - \frac{dL}{dt} = 0, \\ &\frac{\partial L}{\partial s} + \frac{\partial}{\partial s}\left(\frac{\partial L}{\partial \varphi'}\varphi'\right) + \frac{\partial}{\partial t}\left(\frac{\partial L}{\partial \dot{\varphi}}\varphi'\right) - \frac{dL}{ds} = 0. \end{aligned} \tag{2.6}$$

These balance equations are a consequence of the Euler–Lagrange field equations along smooth solutions, i.e., a smooth solution of (2.5) necessarily verifies (2.6). Equivalently, this means that the horizontal equations are implied by the vertical equations; see [2](§5.3), for a proof. However, this is no longer true along nonsmooth solutions and in the discrete case. Considering horizontal variations will become crucial in these cases, as illustrated later in Theorems 2.1 and 3.1.

2.2. Field theoretic setting for nonsmooth problems

While the Euler–Lagrange field equations and the balance equations characterize the critical points of the action functional $\mathfrak{S}$ defined on a space $\mathcal{C}$ of smooth configurations, the treatment of nonsmooth problems requires first and foremost an *appropriate space of configurations with singularities*. We follow the approach taken in [36].

Configuration spaces $\mathcal{C}^{\mathrm{I}}$ and $\mathcal{C}^{\mathrm{II}}$. Assume a codimension one submanifold $\mathrm{D} \subset U$, called the *singularity submanifold*, across which the field ϕ may have singularities. The space $\mathcal{C}^{\mathrm{I}}$ of configurations which are continuous but nonsmooth on D is defined by

$$\begin{aligned} \mathcal{C}^{\mathrm{I}} := \big\{&\phi : U \to X \times M \mid \phi_X : U \to X \text{ is a smooth embedding,} \\ &\phi \text{ is } C^0 \text{ in } U \text{ and of class } C^2 \text{ in } U\backslash\mathrm{D}\big\}. \end{aligned} \tag{2.7}$$

This space of configuration is used, for example, to describe the motion of a geometrically exact beam model with impact on a plane, see Fig. 5.1.

For the collision of two elastic beams (see Fig. 4.1), another configuration space $\mathcal{C}^{\mathrm{II}}$ is needed. Recall that, in this case, $U = [0, 1] \times ([0, L_A] \sqcup [0, L_B])$. The singularity submanifold is thus given by $\mathrm{D} = \mathrm{D}_1 \sqcup \mathrm{D}_2$ with D_1 a codimension one submanifold of $[0, 1] \times [0, L_A]$ and D_2 a codimension one submanifold of $[0, 1] \times [0, L_B]$. The space of configuration fields is now defined by

$$\mathcal{C}^{\mathrm{II}} := \big\{\phi : U \to X \times M \mid \phi_X : U \to X \text{ is a smooth embedding,}$$
$$\phi \text{ is } C^0 \text{ in } U \text{ and of class } C^2 \text{ in } U\backslash\mathrm{D} \text{ and } \phi(\mathrm{D}_1) = \phi(\mathrm{D}_2)\big\}. \tag{2.8}$$

Note that the configuration field $\phi \in \mathcal{C}^{\mathrm{II}}$ contains two maps $\phi_1 := \phi|_{U_1}$ and $\phi_2 := \phi|_{U_2}$, where $U_1 := [0, 1] \times [0, L_A]$, $U_2 := [0, 1] \times [0, L_B]$. These maps correspond to the configuration of each of the two elastic bodies.

The domain D_X where the deformation φ (see Def. (2.1)) may have singularities, is given by

$$\mathrm{D}_X := \phi_X(\mathrm{D}). \tag{2.9}$$

The action functional $\mathfrak{S}^{ns}$. Given a Lagrangian density $\mathcal{L}(t, s, \varphi, \partial_t\varphi, \partial_t\varphi)$, the action functional is given exactly as in the smooth case by (2.4)—except that now, it is defined on one of the two configuration spaces $\mathcal{C}^{\mathrm{I}}$ and $\mathcal{C}^{\mathrm{II}}$.

The inequality constraints Ψ. The *impenetrability constraint* C between the two bodies is described via continuously differentiable functions $\Psi = (\psi^1, \dots, \psi^s) : M \to \mathbb{R}^s$, as $\mathrm{C} = \Psi^{-1}(P)$, with $P := \{(d^1, \dots, d^s) \in \mathbb{R}^s \mid d^1 \leq 0, \dots, d^s \leq 0\}$, where we assume that 0 is a regular value of Ψ. The *contact submanifold* $\partial\mathrm{C}$ is defined by

$$\partial\mathrm{C} := \Psi^{-1}(0). \tag{2.10}$$

Although a general treatment is possible, we assume, for simplicity, that $M = \mathbb{R}^p$ and it is endowed with the standard inner product, and that C is the closure of an open subset of M. Note that the inequality constraints act on the vertical trajectories φ (described by Euler–Lagrange equations (2.5)), and not on the horizontal trajectories ϕ_X (balance of energy and of configurational forces (2.6)).

2.3. Generalized Lagrange multipliers

We now provide the necessary conditions for the critical configurations ϕ of the action functional $\mathfrak{S}^{ns}(\phi)$, subject to the constraints $\varphi(t, s) \in \mathrm{C}$ for all (t, s). These conditions are obtained via the *generalized Lagrange multiplier* approach to enforce inequality constraints (see, e.g., [37,41–43]). Following [21] (Theorem 3), we find:

Theorem 2.1. *Consider a Lagrangian density $\mathcal{L} = \mathcal{L}(t, s, \varphi, \partial_t\varphi, \partial_s\varphi)$, with the same assumptions on the impenetrability constraint $\mathrm{C} = \Psi^{-1}(P)$ as in Section 2.2. If ϕ is a critical point of $\mathfrak{S}^{ns}(\phi)$ relative to the "basic constraint qualification",*[1] *then:*

- *Away from the singularity, the field ϕ satisfies the Euler–Lagrange field equations (2.5), i.e.,*

$$\frac{\partial}{\partial t}\frac{\partial \mathcal{L}}{\partial \dot{\varphi}} + \frac{\partial}{\partial s}\frac{\partial \mathcal{L}}{\partial \varphi'} - \frac{\partial \mathcal{L}}{\partial \varphi} = 0 \quad \text{on } U_X\backslash\mathrm{D}_X \tag{2.11}$$

  together with the balance of energy and configurational forces (2.6) on $U_X\backslash\mathrm{D}_X$.
- *At the singularity D_X, the field ϕ verifies the following two conditions:*
  (a) *the vertical jump condition*

$$\left[\!\left[\frac{\partial L}{\partial \varphi^A{}_{,\mu}}(x)\right]\!\right] N_\mu(x) = \sum_{l=1}^{s} \lambda_l(x)\psi^l{}_{,A}(\varphi(x)), \quad \text{for all } A, \quad \text{on } \mathrm{D}_X, \tag{2.12}$$

  where $\lambda_l(x) < 0$ if $x \in \mathrm{D}_X$ and $\psi^l(\varphi(x)) = 0$. Elsewhere, we have $\lambda_l(x) = 0$. Here $\sum_{l=1}^{s} \lambda_l(x)\psi^l{}_{,A}(\varphi(x))$ is the normal cone at $\varphi(x)$ obtained through the gradient of the constraints acting on the vertical trajectories.

[1] See in p. 198 [43] for the definition of the "basic constraint qualification", which is close in spirit to the linear independence condition on the vectors $\{\nabla\psi^l\}_{l=1,\dots,s}$.

(b) *the horizontal jump condition*

$$\left[\!\left[L\delta^{\mu}_{\nu} - \frac{\partial L}{\partial \varphi^{A}{}_{,\mu}}\varphi^{A}_{,\nu} \right]\!\right] N_{\mu} = 0, \quad \textit{for all } \nu, \quad \textit{on } \mathrm{D}_X \tag{2.13}$$

which imposes the conservation of energy and of configurational forces at the time and position of contact.

In Eqs. (2.12) and (2.13), index μ runs over all the spacetime coordinates t and s in X while index A enumerates the coordinates of the embedding space M. The notation N_μ refers to the normal vector field to the singularity submanifold D_X, and the *jump* $[\![\cdot]\!]$ is defined as the difference between the values on each side of the singularity submanifold D_X.[2] We refer to [36] and [21] for the derivation of these jump terms in the unconstrained and constrained cases.

3. Variational integrators for nonsmooth mechanics

We now derive a variational integrator for nonsmooth continuum mechanics based on a discrete version of the variational formulation presented above. This integrator can be seen as an extension of several earlier variational integrators: in the absence of constraints, the resulting numerical scheme recovers the multisymplectic integrator derived in [31]; in the particular case of classical nonsmooth mechanics (i.e., when spacetime reduces to time), our integrator recovers the variational integrator for collisions of Fetecau, Marsden, Ortiz, West [44].

Besides the use of the generalized Lagrangian multiplier approach in the discrete variational setting, a crucial aspect of our approach is also to consider the *variations of the spacetime mesh* (i.e., discrete horizontal variations), since this naturally yields an additional equation for energy conservation during the impact. Note that discrete horizontal variations have also been considered, for instance, in [2] to construct asynchronous variational integrators.

3.1. Discrete field theoretic description

We now consider a discretization of the field theoretic setting of Section 2.2 based on a rectangular spacetime grid. The discrete version of the spacetime domain U is $U_d = \{0, \dots, N\} \times \{0, \dots, A\}$, where $N+1$ and $A+1$ are the number of temporal and spatial grid points, respectively. We denote by $\square^j_a$ the rectangle given by the four pairs of indices

$$\square^j_a := ((j,a),(j+1,a),(j,a+1),(j+1,a+1))$$

for $j = 0, \dots, N-1$ and $a = 0, \dots, A-1$. The set of all such rectangles is denoted as $U^{\square}_d$.

The discrete configuration is the map

$$\begin{aligned} \phi_d : \quad U_d &\to X \times M && (3.1)\\ (j,a) &\mapsto \phi^j_a := \phi_d(j,a) = \big(\phi_{X_d}(j,a), \varphi_d(\phi_{X_d}(j,a))\big), && (3.2) \end{aligned}$$

where $\phi_{X_d} : U_d \to X, \quad (j,a) \mapsto (j\Delta t, a\Delta s)$, called the *discrete base-space configuration*, encodes the current grid configuration, see Fig. 3.1. In the discrete setting, it is crucial to select an appropriate class of allowable discrete base space configuration ϕ_{X_d}. Note that the knowledge of the discrete configuration ϕ_d induces the couple of maps (ϕ_{X_d}, φ_d).

The discrete configuration spaces $\mathcal{C}^{\mathrm{I}}_d$. In the discrete nonsmooth case, the discrete version of the domain U is $U_d = \{0, \dots, i-1, \tilde{\imath}, i, \dots, N\} \times \{0, \dots, A\}$, where $\tilde{\imath}$ is the time index of the contact time. Given fixed space and time steps Δs and Δt, the discrete base space configuration $\phi_{X_d} : U_d \to X = [0,T] \times [0,L]$ is defined by

$$\begin{aligned} \phi_{X_d}(j,a) &= (j\Delta t, a\Delta s) =: (t^j, s_a) \in X \\ \phi_{X_d}(\tilde{\imath},a) &= (\widetilde{t}, a\Delta s) =: (\widetilde{t}, s_a) \in X, \quad \text{with} \quad (i-1)\Delta t \le \widetilde{t} < i\Delta t. \end{aligned} \tag{3.3}$$

[2] More precisely, given two 2-forms $\alpha^{\pm} \in \Omega^n\left(\overline{U^{\pm}_X}\right)$, the associated jump is defined by $[\![\alpha]\!](x) := \alpha^+(x) - \alpha^-(x)$, for $x \in \mathrm{D}_X$, where the one-dimensional submanifold D_X is oriented according to the orientation inherited from the boundary orientation of ∂U^+_X, via Stokes' theorem. Let dv_{D_X} be the line element on D_X induced by the Riemannian area form on U_X. Therefore, there is a smooth function f on D_X such that $[\![\alpha]\!] = [\![f]\!]\, dv_{\mathrm{D}_X}$.

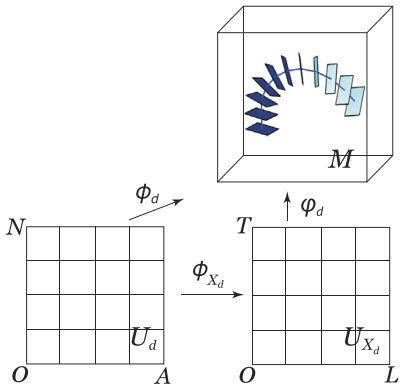

Fig. 3.1. Finite-dimensional domains U_d, U_{X_d}, and M, along with the maps ϕ_{X_d}, ϕ_d, and φ_d used for a 1D + time impact problem.

The first equality indicates that we impose the spacetime sampling to be at least a rectangular grid. The second equality involves the time of contact $\widetilde{t}$ which falls between two regular time steps. It can also be equivalently given by a parameter $\alpha \in [0, 1[$ such that $\tilde{t} := \alpha t^i + (1-\alpha)t^{i-1}$. This is the only additional degree of freedom allowed on the spacetime mesh, and it will be used to get horizontal variations.

The set of all discrete configurations $\phi_d : U_d \to X \times M$ with a discrete base space configuration of the form (3.3) is denoted as $\mathcal{C}_d^{\mathrm{I}}$. In addition to the rectangles $\square_a^j = ((j,a),(j+1,a),(j,a+1),(j+1,a+1))$, we also denote by $\square_a^{i-1}$ and $\widetilde{\square}_a$ the rectangles given by

$$\square_a^{i-1} := ((i-1,a),(\tilde{\imath},a),(i-1,a+1),(\tilde{\imath},a+1))$$
$$\widetilde{\square}_a := ((\tilde{\imath},a),(i,a),(\tilde{\imath},a+1),(i,a+1)).$$

Finally, we denote by φ_a^j and $\widetilde{\varphi}_a$ the values of the field at the spacetime nodes (j,a) and $(\tilde{\imath},a)$.

The constraint $\mathrm{C} = \Psi^{-1}(P)$ on the discrete field then reads

$$\varphi_a^j \in \mathrm{C}, \quad \forall (j,a) \in U_d \tag{3.4}$$

and

$$u \in U_d, \quad \phi_d(u) \in \partial\mathrm{C} \quad \Rightarrow \quad u = (\tilde{\imath},a). \tag{3.5}$$

A node a such that $\phi_d(\tilde{\imath},a) \in \partial\mathrm{C} = \Psi^{-1}(0)$ is said to be in *contact at time* $\tilde{t}$; we also assign time $\tilde{t}$ to all the other spatial nodes to enforce multisymplecticity. We thus define the subset

$$\mathrm{D}_d := \{\tilde{\imath}\} \times \{0,\dots,A\} \subset U_d \tag{3.6}$$

of all the spacetime coordinates of the nodes at the contact time $\widetilde{t}$, see Fig. 3.2. (Note that D_d is not the discrete analogue of the singularity subset D in the continuous case.)

The discrete configuration spaces $\mathcal{C}_d^{\mathrm{II}}$. In the case of the longitudinal impact of two colliding beams, the discrete version of the domain U has now the form

$$U_d = \{0,\dots,i-1,\tilde{\imath},i,\dots,N\} \times (\{0,\dots,A\} \sqcup \{0,\dots,B\}) \ni (j,a,b).$$

The associated rectangles are denoted as $\square_a^j$, $\widetilde{\square}_a$ and $\square_b^j$, $\widetilde{\square}_b$. The subset D_d becomes $\mathrm{D}_d := \{\tilde{\imath}\} \times (\{0,\dots,A\} \sqcup \{0,\dots,B\})$. A discrete configuration is given, as before, by a map

$$\phi_d : U_d \to X \times M,$$

where $X = [0,T] \times ([0,L_A] \sqcup [0,L_B])$.

Given fixed space and time steps Δs and Δt, the discrete base space configuration $\phi_{X_d} : U_d \to X$ is defined by

$$\begin{aligned} \phi_{X_d}(j,a,b) &= (j\Delta t, a\Delta s, b\Delta s) =: (t^j, s_a, s_b) \in X \\ \phi_{X_d}(\tilde{\imath},a,b) &= (\widetilde{t}, a\Delta s, b\Delta s) \in X, \quad \text{with } t^{i-1} \le \widetilde{t} < t^i. \end{aligned} \tag{3.7}$$

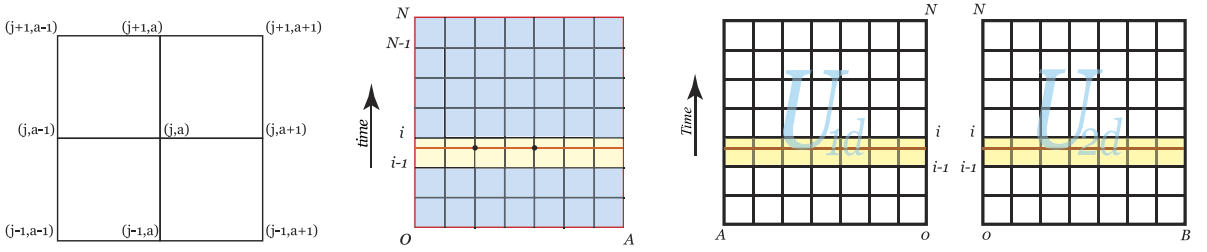

Fig. 3.2. Left: the rectangles $\square_a^j, \square_a^{j-1}, \square_{a-1}^j, \square_{a-1}^{j-1}$. Middle: configuration space $\mathcal{C}_d^{\mathrm{I}}$, with U_d and the discrete spacetime contact sets D_d (yellow), where the nodes in contacts are marked with a bold point. Right: configuration space $\mathcal{C}_d^{\mathrm{II}}$, with $U_d = U_{1d} \cup U_{2d}$ and the discrete spacetime contact sets $\mathrm{D}_d = \mathrm{D}_{1d} \cup \mathrm{D}_{2d}$ (yellow).

The first equality indicates that we impose a rectangular spacetime grid of samples for each body. The second equality involves the time of contact of the two bodies. As before, this time of contact can be equivalently written as a parameter $\alpha \in [0, 1[$ such that $\tilde{t} = \alpha t^i + (1-\alpha)t^{i-1}$.

Let $\mathcal{C}_d^{\mathrm{II}}$ be the set of all discrete configurations $\phi_d : U_d \to X \times M$ with discrete base space configuration of the form (3.7). It is convenient to also define the discrete parameter spaces $U_{1d} = \{0, \dots, N\} \times \{0, \dots, A\}$, $U_{2d} = \{0, \dots, N\} \times \{0, \dots, B\}$, and the subsets $\mathrm{D}_{1d} = \{\tilde{\imath}\} \times \{0, \dots, A\}$, $\mathrm{D}_{2d} = \{\tilde{\imath}\} \times \{0, \dots, B\}$, so that $U_d = U_{1d} \cup U_{2d}$ and $\mathrm{D}_d = \mathrm{D}_{1d} \cup \mathrm{D}_{2d}$. In the case of the collision of two bodies, the constraint on the discrete field is induced by a constraint subset $\mathrm{C} \subset M \times M$. The constraint on the field is given by

$$\left(\varphi_a^j, \varphi_b^j\right) \in \mathrm{C}, \quad \text{for all } (j, a, b) \in U_d \tag{3.8}$$

and

$$\left(\varphi_a^j, \varphi_b^j\right) \in \partial\mathrm{C} \quad \Rightarrow \quad (j, a, b) \in \mathrm{D}_d, \quad \text{i.e.,} \quad j = \tilde{\imath}. \tag{3.9}$$

The discrete action functional $\mathfrak{S}_d^{ns}$. The discrete Lagrangian is constructed such that the following approximation holds

$$\mathcal{L}_d(\square_a^j, \varphi_a^j, \varphi_a^{j+1}, \varphi_{a+1}^j, \varphi_{a+1}^{j+1}) \approx \int_{\square_a^j} \mathcal{L}(t, s, \varphi(t,s), \partial_t\varphi(t,s), \partial_s\varphi(t,s))\, dt \wedge ds,$$

where $\varphi : X \to M$ is a smooth map interpolating the field values $(\varphi_a^j, \varphi_a^{j+1}, \varphi_{a+1}^j, \varphi_{a+1}^{j+1})$.

Let us consider the case of the discrete configuration space $\mathcal{C}_d^{\mathrm{I}}$; the case of $\mathcal{C}_d^{\mathrm{II}}$ is similar. We define $\mathcal{L}_a^j := \mathcal{L}_d(\square_a^j, \varphi_a^j, \varphi_a^{j+1}, \varphi_{a+1}^j, \varphi_{a+1}^{j+1})$ away from the contact time. Near the contact time, we define

$$\mathcal{L}_a^{i-1} := \mathcal{L}_d(\square_a^{i-1}, \varphi_a^{i-1}, \widetilde{\varphi}_a, \varphi_{a+1}^{i-1}, \widetilde{\varphi}_{a+1}) \quad \text{and} \quad \widetilde{\mathcal{L}}_a := \mathcal{L}_d(\widetilde{\square}_a, \widetilde{\varphi}_a, \varphi_a^i, \widetilde{\varphi}_{a+1}, \varphi_{a+1}^i).$$

The discrete action functional is then

$$\mathfrak{S}_d^{ns}(\phi_d) = \sum_{j=0}^{i-2}\sum_{a=0}^{A-1} \mathcal{L}_a^j + \sum_{a=0}^{A-1} \mathcal{L}_a^{i-1} + \sum_{a=0}^{A-1} \widetilde{\mathcal{L}}_a + \sum_{j=i}^{N-1}\sum_{a=0}^{A-1} \mathcal{L}_a^j, \tag{3.10}$$

where we note that the dependence of $\mathfrak{S}_d^{ns}$ on ϕ_{X_d} arises through the explicit dependence of $\mathcal{L}_d$ on $\square_a^j$. We proceed similarly for the discrete configuration space $\mathcal{C}_d^{\mathrm{II}}$.

3.2. Generalized Lagrange multipliers in the discrete setting

We now explicitly provide the necessary conditions on ϕ_d to be a critical point of $\mathfrak{S}_d^{ns}$ with respect to the constraints (3.4) and (3.5) following [21] (Theorems 5 and 7). We focus on the configuration space $\mathcal{C}_d^{\mathrm{I}}$, the case of $\mathcal{C}_d^{\mathrm{II}}$ being similar.

Theorem 3.1. *Consider a discrete Lagrangian* $\mathcal{L}_d(\square_a^j, \varphi_a^j, \varphi_a^{j+1}, \varphi_{a+1}^j, \varphi_{a+1}^{j+1})$ *and the associated discrete action functional* $\mathfrak{S}_d^{ns}$ *defined in (3.10). If* $\phi_d = (\phi_{X_d}, \varphi_d)$ *is a critical point of* $\mathfrak{S}_d^{ns}$ *relative to the constraints (3.4) and (3.5) which verify the hypotheses of Theorem 2.1, then:*

- *Away from the contact time, the fields* ϕ_{X_d} *and* φ_d *satisfy the discrete Euler–Lagrange (DEL) field equations*

$$D_1\mathcal{L}_a^j + D_2\mathcal{L}_a^{j-1} + D_3\mathcal{L}_{a-1}^j + D_4\mathcal{L}_{a-1}^{j-1} = 0, \quad \text{for all } (j,a) \in U_d \backslash \mathrm{D}_d, \tag{3.11}$$

  where D_i *means derivative with respect to the* i*th component of the Lagrangian.*
- *At the contact time, the fields* ϕ_{X_d} *and* φ_d *verify the following conditions:*
  (a) *energy conservation at the contact time*

$$\sum_{a=0}^{A-1} (D_{\widetilde{t}}\mathcal{L}_a^{i-1} - D_{\widetilde{t}}\widetilde{\mathcal{L}}_a) = 0, \tag{3.12}$$

  (b) *vertical discrete jump condition*

$$D_1\widetilde{\mathcal{L}}_a + D_2\mathcal{L}_a^{i-1} + D_3\widetilde{\mathcal{L}}_{a-1} + D_4\mathcal{L}_{a-1}^{i-1} = \sum_{l=1}^{s} (\mathbb{\lambda}_l)_a \nabla\psi^l(\widetilde{\varphi}_a), \tag{3.13}$$

  for all $a = 0, \ldots, A$, *where* $(\mathbb{\lambda}_l)_a < 0$ *if* $(j,a) \in \widetilde{\mathrm{D}}_d$ *and* $\psi_a^l(\widetilde{\varphi}_a) = 0$. *Elsewhere we have* $(\mathbb{\lambda}_l)_a = 0$.

3.3. Discrete Noether's theorem

It is well known in field theory that for each symmetry of the Lagrangian density there is an associated conservation law; this statement is Noether's theorem. We now recall (following [3]) that such a theorem still holds in the discrete field theoretic context, even in the nonsmooth setting.

Let us consider a symmetry Lie group G. We denote by $m \in M \mapsto g \cdot m \in M$ the action of the Lie group element $g \in G$ on the embedding space M. This action induces an action of the Lie algebra $\mathfrak{g}$ of G, denoted by $m \mapsto \xi \cdot m$, for $\xi \in \mathfrak{g}$. With this action, there are four naturally associated discrete momentum maps

$$J_{\mathcal{L}}^k(\square_a^j) := J_{\mathcal{L}}^k(\square_a^j, \varphi_a^j, \varphi_a^{j+1}, \varphi_{a+1}^j, \varphi_{a+1}^{j+1}) \in \mathfrak{g}^*, \quad k = 1, \ldots, 4, \tag{3.14}$$

where $\mathfrak{g}^*$ is the dual space to $\mathfrak{g}$. These momentum maps are defined for $\xi \in \mathfrak{g}$ by

$$\left\langle J_{\mathcal{L}}^1(\square_a^j), \xi \right\rangle = \left\langle \frac{\partial \mathcal{L}_d}{\partial \varphi_a^j}, \xi \cdot \varphi_a^j \right\rangle, \qquad \left\langle J_{\mathcal{L}}^2(\square_a^j), \xi \right\rangle = \left\langle \frac{\partial \mathcal{L}_d}{\partial \varphi_a^{j+1}}, \xi \cdot \varphi_a^{j+1} \right\rangle,$$
$$\left\langle J_{\mathcal{L}}^3(\square_a^j), \xi \right\rangle = \left\langle \frac{\partial \mathcal{L}_d}{\partial \varphi_{a+1}^j}, \xi \cdot \varphi_{a+1}^j \right\rangle, \left\langle J_{\mathcal{L}}^4(\square_a^j), \xi \right\rangle = \left\langle \frac{\partial \mathcal{L}_d}{\partial \varphi_{a+1}^{j+1}}, \xi \cdot \varphi_{a+1}^{j+1} \right\rangle.$$

We say that the discrete Lagrangian is *invariant under the action of* G if

$$\mathcal{L}_d\big(\square_a^j, g \cdot \varphi_a^j, g \cdot \varphi_a^{j+1}, g \cdot \varphi_{a+1}^j, g \cdot \varphi_{a+1}^{j+1}\big) = \mathcal{L}_d\big(\square_a^j, \varphi_a^j, \varphi_a^{j+1}, \varphi_{a+1}^j, \varphi_{a+1}^{j+1}\big) \quad \forall g \in G.$$

The discrete version of Noether's theorem (see Theorem 4.1 in [3]) asserts that if the discrete Lagrangian $\mathcal{L}_d$ is invariant under the action of G and if ϕ_d satisfies the necessary conditions of Theorem 3.1, then

$$\sum_{\square;\, \square \bigcap \left(\partial U_d'^{\square} \cup \mathrm{D}_d'\right) \neq \varnothing} \left(\sum_{k;\, \square^{(k)} \in \partial U_d' \cup \mathrm{D}_d'} J_{\mathcal{L}_d}^k\left(\square^{(k)}\right) \right) = 0,$$

for any subdomain $U_d' \subset U_d$ and where $\mathrm{D}_d' := \mathrm{D}_d \cap U_d'$. To this "field theoretic" version of Noether's theorem, there is an associated "classical" Noether's theorem, written in terms of $J_{\mathcal{L}_d}^k$ as

$$\begin{aligned} \mathbf{J}^-(\boldsymbol{\varphi}^j, \boldsymbol{\varphi}^{j+1}) &:= -\sum_{a=0}^{A-1} J_{\mathcal{L}_d}^1(\square_a^j) + J_{\mathcal{L}_d}^3(\square_a^j) = constant, \\ \mathbf{J}^+(\boldsymbol{\varphi}^j, \boldsymbol{\varphi}^{j+1}) &:= \sum_{a=0}^{A-1} J_{\mathcal{L}_d}^2(\square_a^j) + J_{\mathcal{L}_d}^4(\square_a^j) = constant, \end{aligned} \tag{3.15}$$

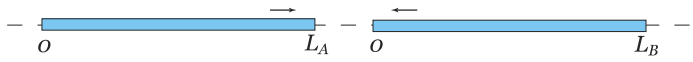

Fig. 4.1. Two one-dimensional beams about to collide.

where $\boldsymbol{\varphi}^j := \left(\varphi_0^j, \varphi_1^j, \ldots, \varphi_A^j\right)$. We refer to Section 3.3 in [3] (for a triangular mesh) and Section 5.1 in [21] for a detailed description of the field theoretic and classical discrete Noether's theorems for variational integrators.

4. Longitudinal impact of two hyperelastic bars

The first illustration of the techniques presented above is the longitudinal impact of two hyperelastic bars.

4.1. Continuous field theoretic setting

We consider the longitudinal impact of two one-dimensional elastic bars, see Fig. 4.1. The deformations of the two bars are described by the two maps $(\varphi_1, \varphi_2) : [0, T] \times \{[0, L_A] \cup [0, L_B]\} \to \mathbb{R}$. The configuration space for this problem is $\mathcal{C}^{\mathrm{II}}$, as defined in (2.8).

The two bars are characterized by their unstretched lengths L_A, L_B [m] (for simplicity, we assume the unstretched length to be equal to the length of the parametrization interval), their masses M_A, M_B [kg/m], their Young's modulus $\mathcal{E}_A$, $\mathcal{E}_B$ [N/m^2], and their cross-sections $\mathcal{S}_A$, $\mathcal{S}_B$ [m^2]. We choose $\mathcal{S}_A = \mathcal{S}_B =: \mathcal{S}$. We assume that both bars are homogeneous and hyperelastic, with stored energy function given by $\frac{1}{2}\mathcal{E}_A\mathcal{S}|\varphi_1' - 1|^2$ and $\frac{1}{2}\mathcal{E}_B\mathcal{S}|\varphi_2' - 1|^2$. The equations of motion are obtained by applying Hamilton's principle $\delta\mathfrak{S} = 0$, for the action functional

$$\mathfrak{S}(\varphi) = \int_0^T \int_0^{L_A} \mathsf{L}_A(\varphi_1, \dot{\varphi}_1, \varphi_1')dsdt + \int_0^T \int_0^{L_B} \mathsf{L}_B(\varphi_2, \dot{\varphi}_2, \varphi_2')dsdt$$

with Lagrangians

$$\mathsf{L}_A(\varphi, \dot{\varphi}, \varphi') = \frac{1}{2}M_A|\dot{\varphi}|^2 - \frac{1}{2}\mathcal{E}_A\mathcal{S}|\varphi' - 1|^2 =: K_A(\dot{\varphi}) - \Phi_A(\varphi'), \tag{4.1}$$

and a similar expression for L_B. The impenetrability constraint reads

$$\psi(t, s_1, s_2, \varphi_1, \varphi_2) = \varphi_2 - \varphi_1 \geqslant 0. \tag{4.2}$$

In the absence of contact, the Euler–Lagrange equations yield the standard equations:

$$M_A\ddot{\varphi}_1 - \mathcal{E}_A\mathcal{S}\varphi_1'' = 0, \qquad M_B\ddot{\varphi}_2 - \mathcal{E}_B\mathcal{S}\varphi_2'' = 0.$$

4.2. Variational integrator for the impact of two bars

We now apply the approach developed in Section 3 to the impact of two elastic bars, i.e., for the configuration space $\mathcal{C}_d^{\mathrm{II}}$. We approximate Eq. (4.1) by the following discrete Lagrangian of order 2, obtained by the generalized trapezoidal rule

$$\begin{aligned}
\mathcal{L}_a^j &= \frac{1}{2}\Delta t^j \Delta s_a \left(K_A(v_a^j) + K_A(v_{a+1}^j) - \left(\Phi_A(e_a^j) + \Phi_A(e_a^{j+1})\right)\right) \\
&= \frac{1}{4}\Delta t^j \Delta s_a M_A \left(\left(\frac{\varphi_a^{j+1} - \varphi_a^j}{\Delta t^j}\right)^2 + \left(\frac{\varphi_{a+1}^{j+1} - \varphi_{a+1}^j}{\Delta t^j}\right)^2\right) \\
&\quad - \frac{1}{4}\Delta t^j \frac{\mathcal{E}_A\mathcal{S}}{\Delta s_a}\left((\varphi_{a+1}^j - \varphi_a^j - \Delta s_a)^2 + (\varphi_{a+1}^{j+1} - \varphi_a^{j+1} - \Delta s_a)^2\right),
\end{aligned} \tag{4.3}$$

where we used the expressions

$$v_a^j := \frac{\varphi_a^{j+1} - \varphi_a^j}{\Delta t^j}, \quad e_a^j := \frac{\varphi_{a+1}^j - \varphi_a^j}{\Delta s_a}.$$

The spacings $\Delta s_a = \ell_A := L_A/A$ and $\Delta s_b = \ell_B := L_B/B$ (for the first, resp. second, bar) are assumed to be constant. The time step sizes Δt^j are constant away from the contact time $\widetilde{t}$ due to our choice of discrete base space configuration (3.7). We thus use the following notation for the time steps:

$$\Delta t^j := \begin{cases} \Delta t & \text{if } j \notin \{i-1, \tilde{\imath}\} \\ \widetilde{t} - t^{i-1} & \text{if } j = i-1 \end{cases} \quad \text{and} \quad \Delta\widetilde{t} := t^i - \widetilde{t}. \tag{4.4}$$

By the choice of the discrete Lagrangian (4.3), each bar is discretized as a mass–spring system with, respectively, stiffness coefficients $k_A := \mathcal{E}_A\mathcal{S}/\ell_A$ and $k_B := \mathcal{E}_B\mathcal{S}/\ell_B$ [N/m], for ℓ_A [m] and ℓ_B [m]. The contact between the extremities φ_A and φ_0 of the two beams (see Fig. 4.1), occurs at time $\widetilde{t}$ when $\varphi_0 - \varphi_A = 0$.

By Theorem 3.1 (corresponding to Theorems 5 and 7 in [21], for the two cases), appropriately modified to treat the case of two elastic bodies, we obtain the following discrete equations:

(i) The DEL field equations away from the contact time

$$\begin{cases} 2\ell_A M_A \left(v_a^j - v_a^{j-1}\right) - (\Delta t^{j-1} + \Delta t^j)\mathcal{E}_A\mathcal{S}\left(e_a^j - e_{a-1}^j\right) = 0, \\ 2\ell_B M_B \left(v_b^j - v_b^{j-1}\right) - (\Delta t^{j-1} + \Delta t^j)\mathcal{E}_B\mathcal{S}\left(e_b^j - e_{b-1}^j\right) = 0, \end{cases} \tag{4.5}$$

for all $j \in \{1, \dots, N-1\}$, $a \in \{1, \dots, A-1\}$, and $b \in \{1, \dots, B-1\}$.

(ii) The discrete zero traction boundary conditions at $a = 0$ and $a = A$

$$\begin{cases} \Delta s_1 M_1 \left(v_0^j - v_0^{j-1}\right) - (\Delta t^{j-1} + \Delta t^j)\mathcal{E}_A\mathcal{S}\left(e_0^j - 1\right) = 0, \\ \Delta s_1 M_1 \left(v_A^j - v_A^{j-1}\right) - (\Delta t^{j-1} + \Delta t^j)\mathcal{E}_A\mathcal{S}\left(1 - e_{A-1}^j\right) = 0, \end{cases} \tag{4.6}$$

for all $j \in \{1, \dots, i-1, i, \dots, N-1\}$. The first equation is also valid for $j = \tilde{\imath}$. Similar boundary conditions are set at $b = 0$ and $b = B$.

(iii) At the contact time $j = \tilde{\imath}$, we obtain

(a) The vertical discrete jump conditions at $a = A$ and $b = 0$

$$\begin{bmatrix} \frac{\ell_A}{2} M_A \left(-\widetilde{v}_A + v_A^{i-1}\right) - \Delta t\, \mathcal{E}_A\mathcal{S}\,(\widetilde{e}_A - 1) \\ \frac{\ell_B}{2} M_B \left(-\widetilde{v}_0 + v_0^{i-1}\right) + \Delta t\, \mathcal{E}_B\mathcal{S}\,(\widetilde{e}_0 - 1) \end{bmatrix} = \lambda_{A,0} \begin{bmatrix} -1 \\ 1 \end{bmatrix}, \tag{4.7}$$

where we modified Eq. (3.13), to take into account the discrete boundary conditions (4.6). When $a \neq A$, and $b \neq 0$ the jump conditions are given by (4.5) and (4.6).

(b) The horizontal discrete jump condition associated to the time component variations, giving the energy conservation during the impact:

$$\sum_{a=0}^{A-1} \left(E_a^{i-1} - \widetilde{E}_a\right) + \sum_{b=0}^{B-1} \left(E_b^{i-1} - \widetilde{E}_b\right) = 0, \tag{4.8}$$

where $E_a^j := -D_{t^j}\mathcal{L}_a^j$ is the energy.

4.3. Numerical tests for two colliding 1D bars

We now present numerical results to validate our approach and compare it to existing methods. In particular, we show that a slight change in the way we handle extremities can dramatically improve the numerical behavior of the simulation.

4.3.1. First discretization of the two bar collision problem

Algorithm. An outline of the simulation algorithm during contact is given below. We note that the principle of the algorithm is quite simple. First, we determine the time of contact. We then apply Theorem 3.1 in order to get the position after contact and the force of reaction at contact.

Contact time integrator 1

(1) If $\psi(t^{j+1}, s_A, s_0, \varphi_A^{j+1}, \varphi_0^{j+1}) < 0$, compute $\alpha\Delta t$, $\alpha \in [0, 1]$, such that $\widetilde{t} = t^j + \alpha\Delta t$ and $\psi(t^j + \alpha\Delta t, s_A, s_0, \widetilde{\varphi}_A, \widetilde{\varphi}_0) = 0$, via Eq. (4.5) and (4.6)
(2) Compute $\widetilde{\varphi}_a$, and $\widetilde{\varphi}_b$, for all a and b, via Eq. (4.5) and (4.6)
(3) Compute φ_a^i and φ_b^i, after contact, when $a \neq A$ and $b \neq 0$
(4) Solve the system of equations (4.7) and (4.8) to compute $\lambda_{A,0}$, φ_A^i, and φ_0^i
(5) Update $t^j = (j+\alpha)\Delta t$, $t^{j+1} = (j+1)\Delta t$, $\varphi_a^j = \widetilde{\varphi}_a$, $\varphi_a^{j+1} = \varphi_a^i$, $\varphi_b^j = \widetilde{\varphi}_b$, and $\varphi_b^{j+1} = \varphi_b^i$

Results. In Fig. 4.2, we present the result of our algorithm (4.5)–(4.8) with the discrete Lagrangian from (4.3), for the longitudinal impact of two identical and non-identical bars with various values for lengths, densities, Young's moduli, discretizations, and speeds of impact. In each case, we observe that the energy is conserved during and after the impact within 0.0001% of the original energy. However, we observe rapid and spurious-looking velocity oscillations during the persistent contact phase as the beams rapidly "bounce off" of each other. While these fine-scale oscillations are to be expected when modeling fully elastic contact of a hyperelastic material model through discrete masses, capturing instead the prolonged contact at a macroscopic scale where the two bar tips remain temporarily "glued" until separation is often desirable. Below, we show that this variant can be achieved by modifying the discrete Lagrangian density near the extremities of the bars, allowing us to obtain a time-averaged velocity while preserving the geometric variational character of our algorithm.

4.3.2. Modified discretization of the two-bar collision problem

We modify the discretization of the bars and the integration steps in order to produce a prolonged contact between the bars for a time period corresponding to the wave propagating to the end the bars and its reflection, i.e., the time necessary for the wave front to emanate from the initial contact in the direction of the extremity of the bar and return to the contact surface—as already studied for small values of the Young's modulus E in [18,38,39].

Modified Lagrangian. Assume that the discrete Lagrangians on the rectangles $\square_{A-1}^j$, and $\square_0^j$ were given by

$$\begin{aligned}
\mathcal{L}_{A-1}^j &= \frac{1}{4}\ell_A M_A \left\{ \frac{(\varphi_{A-1}^{j+1} - \varphi_{A-1}^j)^2}{\Delta t^j} + \frac{(\varphi_A^{j+1} - \varphi_A^j)^2}{\Delta t^j} \right\} \\
&\quad - \frac{1}{4}\Delta t^j k_A \left\{ \left(\varphi_A^j - \varphi_{A-1}^j - \ell_A\right)^2 + \left(\varphi_A^{j+1} - \varphi_{A-1}^{j+1} - \ell_A\right)^2 \right\}, \\
\mathcal{L}_0^j &= \frac{1}{4}\ell_B M_B \left\{ \frac{(\varphi_0^{j+1} - \varphi_0^j)^2}{\Delta t^j} + \frac{(\varphi_1^{j+1} - \varphi_1^j)^2}{\Delta t^j} \right\} \\
&\quad - \frac{1}{4}\Delta t^j k_B \left\{ \left(\varphi_1^j - \varphi_0^j - \ell_B\right)^2 + \left(\varphi_1^{j+1} - \varphi_0^{j+1} - \ell_B\right)^2 \right\},
\end{aligned} \tag{4.9}$$

where $k_A := \mathcal{E}_A\mathcal{S}/\ell_A$ and $k_B := \mathcal{E}_B\mathcal{S}/\ell_B$ are two arbitrary spring stiffness coefficients.

We decompose these two elements and their springs by adding nodes A^- and 0^+ respectively into the intervals $]A-1,\ A[$ and $]0,\ 1[$, thus decomposing the two springs into four springs. In order to induce the *same* potential energy, we adapt the stiffness coefficients, i.e., the spring with stiffness coefficient k_A is replaced by two springs, with stiffness coefficients k_{A1}, k_{A2} and lengths ℓ_{A1}, ℓ_{A2}, which verify

$$\frac{\ell_A}{k_A} = \frac{\ell_{A1}}{k_{A1}} + \frac{\ell_{A2}}{k_{A2}}. \tag{4.10}$$

We proceed in the same manner with the spring of stiffness k_B.

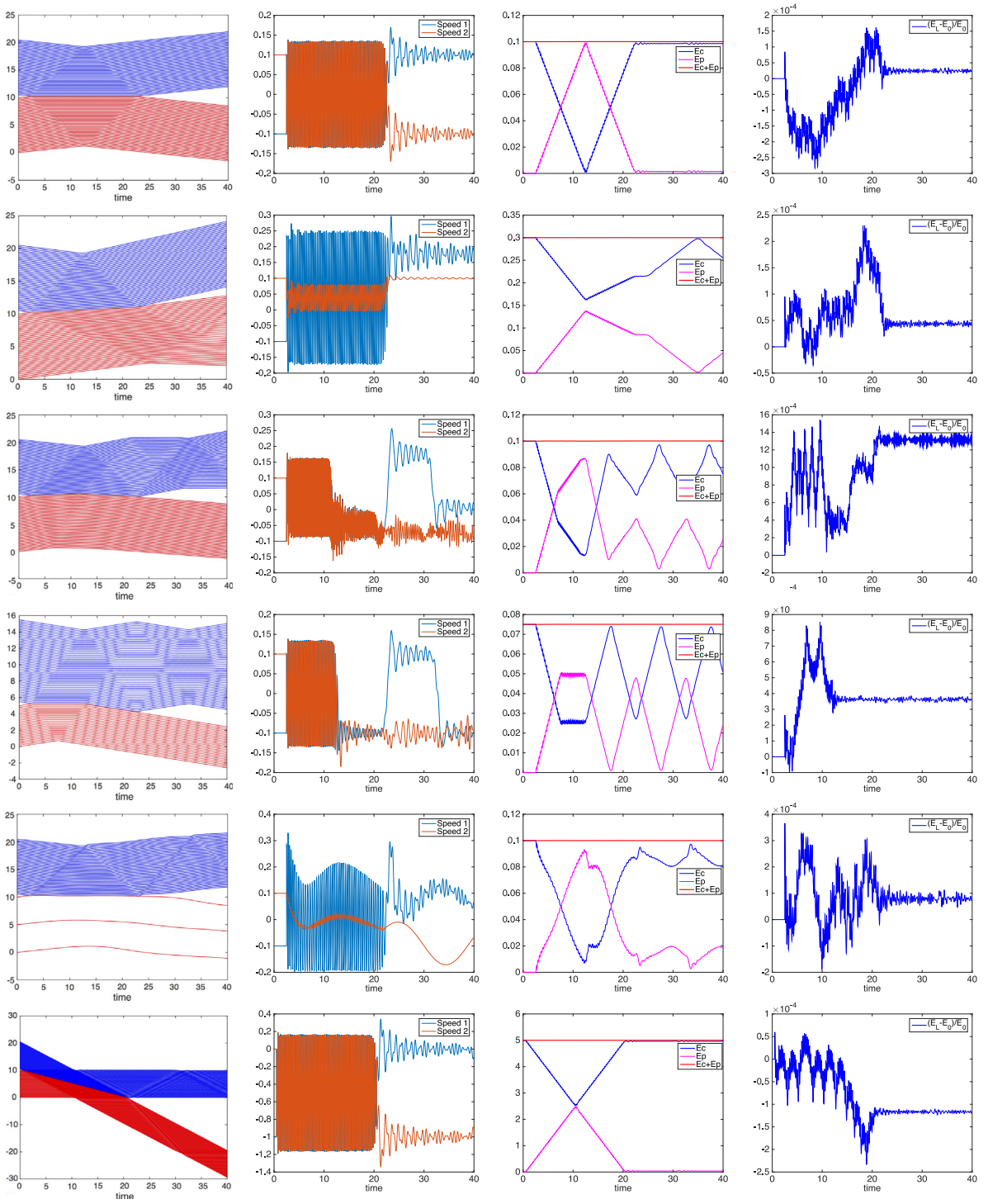

Fig. 4.2. From left to right: displacement, speeds of the nodes in contact, total energy, and relative energy error, for $\Delta t = 0.015$ s and $T = 40$ s. From top to bottom: (1) $L_A = L_B = 10$, $M_A = M_B = 1$, $\mathcal{E}_A = \mathcal{E}_B = 1$, $\ell_A = \ell_B = 0.2$, $v_1 = -0.1$, $v_2 = 0.1$; (2) $L_A = L_B = 10$, $M_A = 1$, $M_B = 5$, $\mathcal{E}_A = \mathcal{E}_B = 1$, $\ell_A = \ell_B = 0.2$, $v_1 = -0.1$, $v_2 = 0.1$; (3) $L_A = L_B = 10$, $M_A = M_B = 1$, $\mathcal{E}_A = 1$, $\mathcal{E}_B = 5$, $\ell_A = \ell_B = 0.2$, $v_1 = -0.1$, $v_2 = 0.1$; (4) $L_A = 10$, $L_B = 5$, $M_A = M_B = 1$, $\mathcal{E}_A = \mathcal{E}_B = 1$, $\ell_A = \ell_B = 0.2$, $v_1 = -0.1$, $v_2 = 0.1$; (5) $L_A = L_B = 10$, $M_A = M_B = 1$, $\mathcal{E}_A = \mathcal{E}_B = 1$, $\ell_A = 0.2$, $\ell_B = 5$, $v_1 = -0.1$, $v_2 = 0.1$; (6) $L_A = L_B = 10$, $M_A = M_B = 1$, $\mathcal{E}_A = \mathcal{E}_B = 1$, $\ell_A = \ell_B = 0.2$, $v_1 = -1$, $v_2 = 0$.

Now, by adding the nodes A^- and 0^+ and modifying the springs but not their masses, we define two new Lagrangians $\mathscr{L}^j_{A-1}$ and $\mathscr{L}^j_0$ as

$$\begin{aligned}
\mathscr{L}^j_{A-1} &:= \frac{1}{4}\ell_A M_A \left\{ \frac{(\varphi^{j+1}_{A-1}-\varphi^j_{A-1})^2}{\Delta t^j} + 0 + \frac{(\varphi^{j+1}_{A}-\varphi^j_{A})^2}{\Delta t^j} \right\} \\
&\quad - \frac{1}{4}\Delta t^j \sum_{i=j}^{j+1} \left\{ k_{A1}\left(\varphi^i_{A^-}-\varphi^i_{A-1}-\ell_{A1}\right)^2 + k_{A2}\left(\varphi^i_{A}-\varphi^i_{A^-}-\ell_{A2}\right)^2 \right\} = \mathcal{L}^j_{A-1}, \\
\mathscr{L}^j_{0} &:= \frac{1}{4}\ell_B M_B \left\{ \frac{(\varphi^{j+1}_{0}-\varphi^j_{0})^2}{\Delta t^j} + 0 + \frac{(\varphi^{j+1}_{1}-\varphi^j_{1})^2}{\Delta t^j} \right\} \\
&\quad - \frac{1}{4}\Delta t^j \sum_{i=j}^{j+1} \left\{ k_{B1}\left(\varphi^i_{0^+}-\varphi^i_{0}-\ell_{B1}\right)^2 + k_{B2}\left(\varphi^i_{1}-\varphi^i_{0^+}-\ell_{B2}\right)^2 \right\} = \mathcal{L}^j_{0}.
\end{aligned} \tag{4.11}$$

Next, we replace the mass matrices $\begin{bmatrix} M_A & 0 & M_A \end{bmatrix}$ and $\begin{bmatrix} M_B & 0 & M_B \end{bmatrix}$ by the mass matrices $\begin{bmatrix} M_A & M_A & 0 \end{bmatrix}$ and $\begin{bmatrix} 0 & M_B & M_B \end{bmatrix}$, respectively, making the nodes in contact massless, thus "virtual". We then get the new Lagrangians $\mathbb{L}^j_{A-1}$ and $\mathbb{L}^j_0$

$$\begin{aligned}
\mathbb{L}^j_{A-1} &:= \frac{1}{4}\ell_A M_A \left\{ \frac{(\varphi^{j+1}_{A-1}-\varphi^j_{A-1})^2}{\Delta t^j} + \frac{(\varphi^{j+1}_{A^-}-\varphi^j_{A^-})^2}{\Delta t^j} + 0 \right\} \\
&\quad - \frac{1}{4}\Delta t^j \sum_{i=j}^{j+1} \left\{ k_{A1}\left(\varphi^i_{A^-}-\varphi^i_{A-1}-\ell_{A1}\right)^2 + k_{A2}\left(\varphi^i_{A}-\varphi^i_{A^-}-\ell_{A2}\right)^2 \right\}, \\
\mathbb{L}^j_{0} &:= \frac{1}{4}\ell_B M_B \left\{ 0 + \frac{(\varphi^{j+1}_{0^+}-\varphi^j_{0^+})^2}{\Delta t^j} + \frac{(\varphi^{j+1}_{1}-\varphi^j_{1})^2}{\Delta t^j} \right\} \\
&\quad - \frac{1}{4}\Delta t^j \sum_{i=j}^{j+1} \left\{ k_{B1}\left(\varphi^i_{0^+}-\varphi^i_{0}-\ell_{B1}\right)^2 + k_{B2}\left(\varphi^i_{1}-\varphi^i_{0^+}-\ell_{B2}\right)^2 \right\},
\end{aligned} \tag{4.12}$$

where the potential energy and the total mass have *not* changed, we only slightly changed the physical discretization of the bars near their tips.

Modified integrator. Away from a contact, the DEL equations at $a = A-1$ and $a = A^-$ become

$$\begin{cases}
2\ell_A M_A \left(v^j_{A-1} - v^{j-1}_{A-1}\right) - (\Delta t^{j-1} + \Delta t^j)\mathcal{S}\left[\mathcal{E}_{A1}(e^j_{A-1}-1) - \mathcal{E}_A(e^j_{A-2}-1)\right] = 0, \\
\ell_A M_A \left(v^j_{A^-} - v^{j-1}_{A^-}\right) + (\Delta t^{j-1} + \Delta t^j)\mathcal{S}\,\mathcal{E}_{A1}(e^j_{A-1}-1) = 0,
\end{cases} \tag{4.13}$$

where $e^j_{A-1} = \left(\varphi^j_{A^-} - \varphi^j_{A-1}\right)/\ell_{A1}$. Similar equations hold at nodes $b = 0^+$ and $b = 1$. These equations thus define our integrator when there is no contact.

When a contact happens, we must proceed as follows:

- At time $\widetilde{t_1}$ denoting the beginning of the prolonged contact, we get from (3.13) by taking into account the fact that the nodes in contact have no mass that

$$\frac{1}{2}k_A\left(\Delta t^{i-1} + \Delta\widetilde{t_1}\right)(\widetilde{\varphi}_A - \widetilde{\varphi}_{A^-} - \ell_{A2}) = \frac{1}{2}k_B\left(\Delta t^{i-1} + \Delta\widetilde{t_1}\right)(\widetilde{\varphi}_{0^+} - \widetilde{\varphi}_0 - \ell_{B1}) = \widetilde{\mathbb{\lambda}}. \tag{4.14}$$

  Since $\widetilde{\varphi}_A - \widetilde{\varphi}_{A^-} - \ell_{A2} = \widetilde{\varphi}_{0^+} - \widetilde{\varphi}_0 - \ell_{B1} = 0$, we get $\widetilde{\mathbb{\lambda}} = 0$. (We get a similar result at the end of the prolonged contact, at time denoted $\widetilde{t_2}$.)

Integration is then obtained via Theorem 3.1, where the energy preservation mentioned in Eq. (3.12) now reads:

$$\sum_{a=0}^{A-2} E_a^{i-1} + \mathbb{E}_{A-1}^{i-1} + \mathbb{E}_0^{i-1} + \sum_{b=1}^{B-1} E_b^{i-1} - \sum_{a=0}^{A-2} \widetilde{E}_a - \sum_{b=1}^{B-1} \widetilde{E}_b$$

$$- \frac{1}{4}\ell_A M_A \left\{ \frac{(\varphi_{A-1}^i - \widetilde{\varphi}_{A-1})^2}{(\Delta\widetilde{t}_1)^2} + \frac{(\varphi_{A^-}^i - \widetilde{\varphi}_{A^-})^2}{(\Delta\widetilde{t}_1)^2} \right\} - \frac{1}{4}\ell_B M_B \left\{ \frac{(\varphi_{0^+}^i - \widetilde{\varphi}_{0^+})^2}{(\Delta\widetilde{t}_1)^2} + \frac{(\varphi_1^i - \widetilde{\varphi}_1)^2}{(\Delta\widetilde{t}_1)^2} \right\}$$

$$- \frac{1}{4}\left\{ k_{A1}\,(\widetilde{\varphi}_{A^-} - \widetilde{\varphi}_{A-1} - \ell_{A1})^2 + k_{B1}\,(\widetilde{\varphi}_{0^+} - \widetilde{\varphi}_0 - \ell_{B1})^2 + k_{AB}\,(\widetilde{\varphi}_{0^+} - \widetilde{\varphi}_{A^-} - \ell_{AB})^2 \right\}$$

$$- \frac{1}{4}\left\{ k_{A1}\left(\varphi_{A^-}^i - \varphi_{A-1}^i - \ell_{A1}\right)^2 + k_{B1}\left(\varphi_{0^+}^i - \varphi_0^i - \ell_{B1}\right)^2 + k_{AB}\left(\varphi_{0^+}^i - \varphi_{A^-}^i - \ell_{AB}\right)^2 \right\} = 0, \quad (4.15)$$

where we used $E_a^j := -D_{t^j}\mathcal{L}_a^j$, in $a = 0, 1, \ldots, A-2$ and $\mathbb{E}_{A-1}^j := -D_{t^j}\mathbb{L}_{A-1}^j$, and for $\ell_{AB} = (\ell_{A2} + \ell_{B1})$, $\ell_{AB}/k_{AB} = \ell_{A2}/k_{A2} + \ell_{B1}/k_{B1}$, and $k_{AB} := \mathcal{E}_{AB}\mathcal{S}/\ell_{AB}$.

- During the prolonged contact (i.e., between time $\widetilde{t}_1$ and a time we denote $\widetilde{t}_2$), we can identify nodes A and 0, that is, the element with extremities A^- and A of the first bar and extremities 0 and 0^+ of the second bar are treated as one single element of the discretization since $\widetilde{\mathbb{N}} = 0$ there.
  Updating the node positions is then given by (4.5) for all $j \in \{1, \ldots, N-1\}$, $a \in \{1, \ldots, A-2\}$, and $b \in \{2, \ldots, B-1\}$, and by (4.6) at $a = 0$ and $b = B$. For the node $a = A-1$ the update is given by (4.13), and for $a = A^-$ we get

$$2\ell_A M_A \left(v_{A^-}^j - v_{A^-}^{j-1}\right) - (\Delta t^{j-1} + \Delta t^j)\mathcal{S}\left[\mathcal{E}_{AB}\left(e_{A^-}^j - 1\right) - \mathcal{E}_{A1}\left(e_{A-1}^j - 1\right)\right] = 0, \quad (4.16)$$

  where $e_{A^-}^j = \left(\varphi_{0^+}^j - \varphi_{A^-}^j\right)/\ell_{AB}$. Similar equations hold at the nodes $b = 0^+$. Note that the intensity of the reaction force $\mathbb{N}$ is obtained by calculating the compression of the spring between A^- and 0^+.
- The end of the prolonged contact happens as soon as $|\varphi_{A^-}^j - \varphi_{0^+}^j| \le \ell_{AB}$ and $|\varphi_{A^-}^{j+1} - \varphi_{0^+}^{j+1}| \ge \ell_{AB}$. When this separation occurs, we calculate its exact time $\widetilde{t}_2 = t^j + \alpha\Delta t$ when the contact ends, corresponding to the time when $|\widetilde{\varphi}_{A^-} - \widetilde{\varphi}_{0^+}| = \ell_{AB}$. Then we proceed just like at the very beginning of the contact, where the energy conservation is now given by

$$\sum_{a=0}^{A-2} \widetilde{E}_a + \widetilde{\mathbb{E}}_{A-1} + \widetilde{\mathbb{E}}_0 + \sum_{b=1}^{B-1} \widetilde{E}_b - \sum_{a=0}^{A-2} E_a^{i-1} - \sum_{b=1}^{B-1} E_b^{i-1}$$

$$- \frac{1}{4}\ell_A M_A \left\{ \frac{(\widetilde{\varphi}_{A-1} - \varphi_{A-1}^{i-1})^2}{(\Delta t^{i-1})^2} + \frac{(\widetilde{\varphi}_{A^-} - \varphi_{A^-}^{i-1})^2}{(\Delta t^{j-1})^2} \right\} - \frac{1}{4}\ell_B M_B \left\{ \frac{(\widetilde{\varphi}_{0^+} - \varphi_{0^+}^{i-1})^2}{(\Delta t^{i-1})^2} + \frac{(\widetilde{\varphi}_1 - \varphi_1^{i-1})^2}{(\Delta t^{i-1})^2} \right\}$$

$$- \frac{1}{4}\left\{ k_{A1}\,(\widetilde{\varphi}_{A^-} - \widetilde{\varphi}_{A-1} - \ell_{A1})^2 + k_{B1}\,(\widetilde{\varphi}_{0^+} - \widetilde{\varphi}_0 - \ell_{B1})^2 + k_{AB}\,(\widetilde{\varphi}_{0^+} - \widetilde{\varphi}_{A^-} - \ell_{AB})^2 \right\}$$

$$- \frac{1}{4}\left\{ k_{A1}\left(\varphi_{A^-}^{i-1} - \varphi_{A-1}^{i-1} - \ell_{A1}\right)^2 + k_{B1}\left(\varphi_{0^+}^{i-1} - \varphi_0^{i-1} - \ell_{B1}\right)^2 + k_{AB}\left(\varphi_{0^+}^{i-1} - \varphi_{A^-}^{i-1} - \ell_{AB}\right)^2 \right\} = 0. \quad (4.17)$$

Remark 4.1. Unlike earlier methods (e.g., [38]), there is *no need to compute or estimate the time of release* based on the physical parameters of the bars: the time of release is obtained directly from (4.5), (4.6) and (4.8) by solving for the position of the nodes in contact. The result is illustrated in Fig. 4.3 where we chose $\ell_{A2} = \ell_A/4$ and $\ell_{B1} = \ell_B/4$.

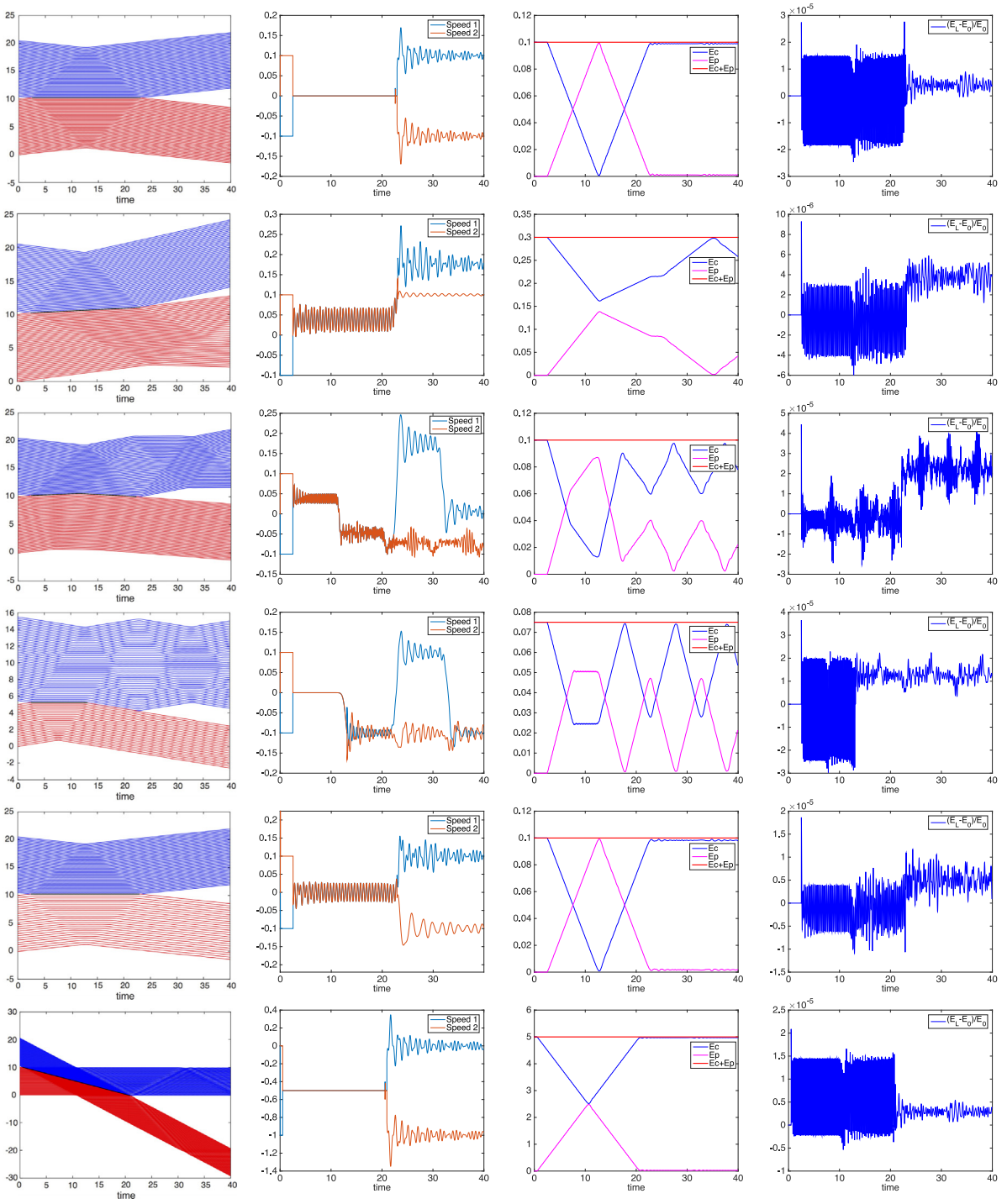

Fig. 4.3. Prolonged contact. From left to right: displacement, speeds of the nodes in contact, total energy, and relative energy error, $\Delta t = 0.015$ s, $T = 40$ s. From top to bottom: (1) $L_A = L_B = 10$, $M_A = M_B = 1$, $\mathcal{E}_A = \mathcal{E}_B = 1$, $\ell_A = \ell_B = 0.2$, $v_1 = -0.1$, $v_2 = 0.1$; (2) $L_A = L_B = 10$, $M_A = 1$, $M_B = 5$, $\mathcal{E}_A = \mathcal{E}_B = 1$, $\ell_A = \ell_B = 0.2$, $v_1 = -0.1$, $v_2 = 0.1$; (3) $L_A = L_B = 10$, $M_A = M_B = 1$, $\mathcal{E}_A = 1$, $\mathcal{E}_B = 5$, $\ell_A = \ell_B = 0.2$, $v_1 = -0.1$, $v_2 = 0.1$; (4) $L_A = 10$, $L_B = 5$, $M_A = M_B = 1$, $\mathcal{E}_A = \mathcal{E}_B = 1$, $\ell_A = \ell_B = 0.2$, $v_1 = -0.1$, $v_2 = 0.1$; (5) $L_A = L_B = 10$, $M_A = M_B = 1$, $\mathcal{E}_A = \mathcal{E}_B = 1$, $\ell_A = 0.2$, $\ell_B = 0.4$, $v_1 = -0.1$, $v_2 = 0.1$; (6) $L_A = L_B = 10$, $M_A = M_B = 1$, $\mathcal{E}_A = \mathcal{E}_B = 1$, $\ell_A = \ell_B = 0.2$, $v_1 = -1$, $v_2 = 0$.

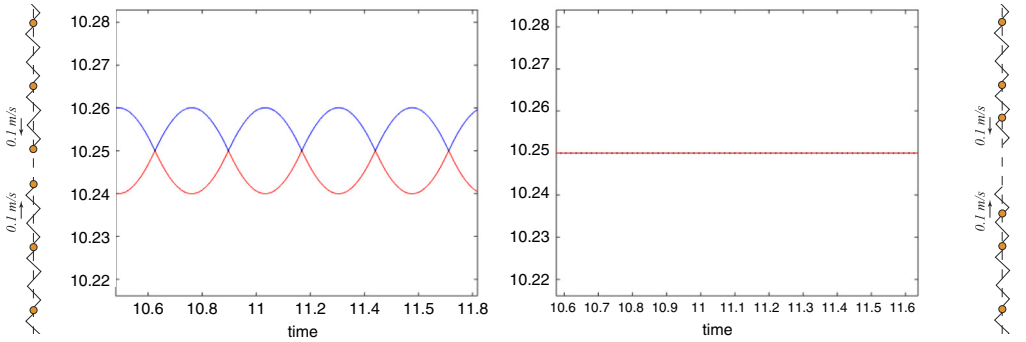

Fig. 4.4. From left to right: trajectories of the nodes at contact, without or with modification of the mass matrix.

Algorithm. A pseudocode of the modified algorithm during contact is given below.

Contact time integrator 2

(**A1**) If $\psi(t^j, s_{A^-}, s_{0^+}, \varphi^j_{A^-}, \varphi^j_{0^+}) > \ell_{AB}$, and $\psi(t^{j+1}, s_{A^-}, s_{0^+}, \varphi^{j+1}_{A^-}, \varphi^{j+1}_{0^+}) < \ell_{AB}$, compute $\alpha\Delta t$, with $\alpha \in [0,1]$, such that $\widetilde{t}_1 = t^j + \alpha\Delta t$ and $\psi(t^j + \alpha\Delta t, s_{A^-}, s_{0^+}, \widetilde{\varphi}_{A^-}, \widetilde{\varphi}_{0^+}) = \ell_{AB}$, via Eq. (4.5) and (4.6)
(2) Compute $\widetilde{\varphi}_a$, and $\widetilde{\varphi}_b$, for all a and b, via Eq. (4.5) and (4.6)
(3) Compute φ^i_a and φ^i_b, after contact, for $a \neq A^-$ and $b \neq 0^+$
(4) Solve the system of equations (4.13) and (4.15), to compute $\varphi^i_{A^-}$ and $\varphi^i_{0^+}$
(5) Update $t^j = (j+\alpha)\Delta t$, $t^{j+1} = (j+1)\Delta t$, $\varphi^j_a = \widetilde{\varphi}_a$, $\varphi^{j+1}_a = \varphi^i_a$, $\varphi^j_b = \widetilde{\varphi}_b$, and $\varphi^{j+1}_b = \varphi^i_b$

(**B1**) Else, if $\psi(t^j, s_{A^-}, s_{0^+}, \varphi^j_{A^-}, \varphi^j_{0^+}) < \ell_{AB}$, and $\psi(t^{j+1}, s_{A^-}, s_{0^+}, \varphi^{j+1}_{A^-}, \varphi^{j+1}_{0^+}) < \ell_{AB}$, we compute φ^{j+1}_a and φ^{j+1}_b via (4.5), (4.6), (4.16), and we update the time $t^{j+1} = (j+1)\Delta t$

(**C1**) Else, if $\psi(t^j, s_{A^-}, s_{0^+}, \varphi^j_{A^-}, \varphi^j_{0^+}) < \ell_{AB}$, and $\psi(t^{j+1}, s_{A^-}, s_{0^+}, \varphi^{j+1}_{A^-}, \varphi^{j+1}_{0^+}) > \ell_{AB}$, compute $\alpha\Delta t$, $\alpha \in [0,1]$, such that $\widetilde{t}_2 = t^j + \alpha\Delta t$ and $\psi(t^j + \alpha\Delta t, s_{A^-}, s_{0^+}, \widetilde{\varphi}_{A^-}, \widetilde{\varphi}_{0^+}) = \ell_{AB}$, via Eq. (4.5) and (4.6)
(2) Compute $\widetilde{\varphi}_a$, and $\widetilde{\varphi}_b$, for all a and b, via Eq. (4.5) and (4.6)
(3) Compute φ^i_a and φ^i_b, after contact, when $a \neq A^-$ and $b \neq 0^+$
(4) Solve the system of equations (4.16), and energy conservation (4.17) to compute $\varphi^i_{A^-}$ and $\varphi^i_{0^+}$
(5) Update $t^j = (j+\alpha)\Delta t$, $t^{j+1} = (j+1)\Delta t$, $\varphi^j_a = \widetilde{\varphi}_a$, $\varphi^{j+1}_a = \varphi^i_a$, $\varphi^j_b = \widetilde{\varphi}_b$, and $\varphi^{j+1}_b = \varphi^i_b$

Note that the algorithm is slightly different from the previous one. First, we determine the time of contact. Then, at time of contact, we get the position after contact through conservation of energy. Then, as long as the bars remain in contact, we calculate the new position through a variational integrator for a coupled oscillator. The bars will naturally separate at some point.

Results. First, note that Fig. 4.3 matches Fig. 4.2 very well in terms of displacements and energy for all the tests, but the fast-scale oscillations during the prolonged contact have disappeared. The total energy is conserved during and after impact within 0.00002%, and the momentum is conserved to within machine accuracy.

Note however that changing the size of the last elements of the bars renders the choice of a time step a bit more difficult: enforcing Courant condition requires potentially much smaller time steps. A proper treatment of contact problems would thus require a graded refinement at the end of the bars and an adaptive time stepping approach to efficiently deal with the collision with guaranteed stability. Finally, Fig. 4.4 illustrates the two different behaviors of the nodes at contact for our two different integrators.

Comparison with earlier results. Capturing the persistent contact between colliding bodies is known to be a challenge in the simulation of elastic impact problems. Many approaches have been developed in order to consistently reproduce this physical phenomenon, mostly through the introduction of additional constraints in order to closely match the expected behavior. In [38], for instance, the release conditions were computed based on the speed of sound of each body. The quality of these approximations was improved in [12,39,45]. More recently, in [18], some features of the variational (*in time*) framework of nonsmooth classical mechanics were used, in order to derive new explicit

algorithms for finite element simulations of solids and shells. This is in stark contrast to our approach, which is *fully variational in space and time*, with the consequence that the energy and momentum are automatically preserved over the whole simulation. Moreover, contrary to the results in [18] Figs. 8 & 9, we obtain a zero velocity for the nodes at contact, see Figs. 4.3 and 4.4. For the study of impact of other shapes, e.g., cubes and hexagonal cylinders, see [20].

5. Impact of a geometrically exact beam on a plane

We now consider the impact of a geometrically exact beam [40] in $\mathbb{R}^3$ with a fixed planar obstacle. The configuration space for this problem is the space $\mathcal{C}^{\mathrm{I}}$ defined in (2.7). The position of a geometrically exact beam consists of a family of planar cross-sections (compact domains) $\mathcal{S}(s)$, $s \in [0, L]$, defined by rotation matrices $[0, L] \ni s \mapsto \Lambda(s) \in SO(3)$, and connected by the line of centroids $[0, L] \ni s \mapsto \mathbf{r}(s) = (z^1, z^2, z^3) \in \mathbb{R}^3$. For a given orthonormal basis $\{\mathbf{E}_i\}_{i=1,2,3}$ of $\mathbb{R}^3$, $\{\Lambda(s)\mathbf{E}_i\}_{i=1,2,3}$ is also an orthonormal basis of $\mathbb{R}^3$ for any $s \in [0, L]$, adapted to the position of the beam, i.e., $\{\Lambda(s)\mathbf{E}_1, \Lambda(s)\mathbf{E}_2\}$ form an orthonormal basis of the planar cross-section $\mathcal{S}(s)$ and $\Lambda(s)\mathbf{E}_3$ is the unit normal to $\mathcal{S}(s)$. Let (ℓ_1, ℓ_2) denote the coordinates in $\mathcal{S}(s)$ relative to $\{\Lambda(s)\mathbf{E}_1, \Lambda(s)\mathbf{E}_2\}$. Thinking of the beam in the reference configuration as $\mathcal{A} \times [0, L] \subset \mathbb{R}^3$, $\mathcal{A}$ being a compact connected subset in $\mathbb{R}^2$, an admissible configuration $f : \mathcal{A} \times [0, L] \to \mathbb{R}^3$ of the beam is of the form

$$\mathbf{x} = f(\ell_1, \ell_2, s) = \mathbf{r}(s) + \sum_{\alpha=1}^{2} \ell_\alpha \Lambda(s)\mathbf{E}_\alpha.$$

5.1. Field theoretic setting

The field theoretic description of the convective representation of geometrically exact beams is given in [46]. The deformation field φ reads

$$[0, T] \times [0, L] \ni (t, s) \longmapsto \varphi(t, s) = (\Lambda(t, s), \mathbf{r}(t, s)) \in SE(3),$$

and takes values in the special Euclidean group $SE(3)$ whose elements are orientation preserving rigid motions in space.

The Lagrangian density $\mathcal{L}(t, s, \varphi, \dot{\varphi}, \varphi') = \mathcal{L}(t, s, \Lambda, \mathbf{r}, \dot{\Lambda}, \dot{\mathbf{r}}, \Lambda', \mathbf{r}')$ of a geometrically exact beam is best expressed using convective variables. Given the field $g(t, s) := (\Lambda(t, s), \mathbf{r}(t, s)) \in SE(3)$, the convective velocities are $\xi := (\omega, \boldsymbol{\gamma}) := (\Lambda^{-1}\dot{\Lambda}, \Lambda^{-1}\dot{\mathbf{r}}) = g^{-1}\dot{g} \in \mathfrak{se}(3)$ and the convective strains are $\eta := (\Omega, \boldsymbol{\Gamma}) := (\Lambda^{-1}\Lambda', \Lambda^{-1}\mathbf{r}') = g^{-1}g' \in \mathfrak{se}(3)$, where $\mathfrak{se}(3)$ denotes the Lie algebra of $SE(3)$. With these convective variables, the Lagrangian density is expressed as

$$\begin{aligned} \mathcal{L}(\Lambda, \mathbf{r}, \boldsymbol{\omega}, \boldsymbol{\gamma}, \boldsymbol{\Omega}, \boldsymbol{\Gamma}) &= \frac{1}{2}\langle \mathbb{J}\xi, \xi\rangle - \frac{1}{2}\langle \mathbb{C}(\eta - \mathbf{E}_6), (\eta - \mathbf{E}_6)\rangle - \Pi(g) \\ &=: K(\xi) - \Phi(\eta) - \Pi(g), \end{aligned} \tag{5.1}$$

where $\mathbf{E}_6 = (0, 0, 0, 0, 0, 1) \in \mathbb{R}^6$, $\langle\,,\,\rangle$ is the usual inner product on $\mathbb{R}^6$, $K(\xi)$, $\Phi(\eta)$, and $\Pi(g)$ are, respectively, the kinetic energy density, the strain energy density, and the external (such as gravitational) potential energy density. The bold letters $\boldsymbol{\omega}$, $\boldsymbol{\gamma}$ are the images of the same letters in a lighter font under the standard isomorphism $\mathfrak{se}(3) \cong \mathbb{R}^6$ given by

$$\mathfrak{se}(3) = \mathfrak{so}(3) \times \mathbb{R}^3 \ni (\omega, \boldsymbol{\gamma}) \longmapsto (\boldsymbol{\omega}, \boldsymbol{\gamma}) \in \mathbb{R}^6, \qquad \widehat{\boldsymbol{\omega}} = \omega,$$

where $\widehat{\boldsymbol{\omega}}\mathbf{v} := \boldsymbol{\omega} \times \mathbf{v}$ for any $\mathbf{v} \in \mathbb{R}^3$. In (5.1), K, Φ, and Π denote the kinetic energy density, the bending energy density, and the potential energy density, respectively. The 6×6 matrix $\mathbb{J}$ is given by

$$\mathbb{J} := \begin{bmatrix} J & 0 \\ 0 & M\mathbf{I}_3 \end{bmatrix}, \tag{5.2}$$

where $M = \rho|\mathcal{S}| \in \mathbb{R}$ is the mass by unit of length of the beam, ρ is the mass density, $|\mathcal{S}|$ is the area of the cross section, $\mathbf{I}_3$ is the identity 3×3 matrix, and $J := \mathrm{diag}\,(I_1, I_2, I_1 + I_2)$ is the diagonalized inertia tensor of the beam, with I_1 and I_2 the principal moments of inertia of $\mathcal{S}(s)$ and $I = I_1 + I_2$ its polar moment of inertia. The model we

consider assumes a beam formed by a homogeneous material whose cross-sections $\mathcal{S}(s)$ are all identical to $\mathcal{S}(0)$. In particular, the areas of all the cross-sections and their moments of inertia are independent of (t, s). Consequently, the 6×6 matrix $\mathbb{C}$ encoding the potential interaction is given by

$$\mathbb{C} := \begin{bmatrix} \mathbf{C}_2 & 0 \\ 0 & \mathbf{C}_1 \end{bmatrix}, \tag{5.3}$$

where the constant matrices $\mathbf{C}_1, \mathbf{C}_2$ are of the form

$$\mathbf{C}_1 := \operatorname{diag}(G|\mathcal{S}| \;\; G|\mathcal{S}| \;\; E|\mathcal{S}|) \quad \text{and} \quad \mathbf{C}_2 := \operatorname{diag}(EI_1 \;\; EI_2 \;\; GI), \tag{5.4}$$

with E the Young's modulus, $G := E/[2(1+\nu)]$ the shear modulus, and ν the Poisson ratio (see [47]).

Hamilton's principle in convective variables reads

$$\delta \int_0^T (K(\xi(t,s)) - \Phi(\eta(t,s)) - \Pi(g(t,s)))\, dtds = 0$$

for appropriately constrained variations (see [46]), resulting in the Euler–Lagrange field equations for the geometrically exact beam that are compactly written as

$$\frac{\partial}{\partial t}\mathbb{J}\xi - \operatorname{ad}^*_\xi \mathbb{J}\xi = \frac{\partial}{\partial s}\frac{\partial \Phi}{\partial \eta} - \operatorname{ad}^*_\eta \frac{\partial \Phi}{\partial \eta} - g^{-1}\frac{\partial \Pi}{\partial g}, \tag{5.5}$$

together with the zero traction boundary condition $\frac{\partial \Phi}{\partial \eta} = 0$ at the boundaries $s = 0$ and $s = L$. We used above the coadjoint action of $\mathfrak{se}(3)$ given by $\operatorname{ad}^*_{(\boldsymbol{\omega},\boldsymbol{\gamma})}(\boldsymbol{\mu}, \boldsymbol{\nu}) := -(\boldsymbol{\omega} \times \boldsymbol{\mu} + \boldsymbol{\gamma} \times \boldsymbol{\nu}, \boldsymbol{\omega} \times \boldsymbol{\nu})$, where we recall that $\xi := (\boldsymbol{\omega}, \boldsymbol{\gamma})$ and $\eta := (\boldsymbol{\Omega}, \boldsymbol{\Gamma})$.

The plane impacted by the beam is defined by the equation $z^3 = 0$ and we choose the impenetrability condition $\psi : SE(3) \to \mathbb{R}$ given by

$$\psi(\Lambda, \mathbf{r}) = \langle \mathbf{r}(t,s), \mathbf{E}_3 \rangle \geqslant 0. \tag{5.6}$$

This choice assumes that we take into account only the configuration of the centroid to impose the impenetrability constraint. The constraint subdomain is

$$\begin{aligned} \mathrm{C} &:= \{(\Lambda, \mathbf{r}) \in SE(3) \mid -\psi(\Lambda, \mathbf{r}) \in]-\infty, 0]\} \\ &= -\psi^{-1}(]-\infty, 0]) = SO(3) \times \{(z^1, z^2, z^3) \mid z^3 \geq 0\}. \end{aligned} \tag{5.7}$$

Note that, in this case, only the translational part of the Lie group $SE(3)$ appears in the constraints.

A note about symmetry. The potential energy Π is defined as the gravitational potential energy density along the axis $\mathbf{E}_3$. The Lagrangian is invariant with respect to the subgroup of $SE(3)$ defined by rotations around the vertical axis and by translations that are parallel to the plane $z_3 = 0$. To this symmetry is associated a field theoretic momentum map via Noether's theorem. We shall see later that the discrete Lagrangian inherits this symmetry, thus yielding a discrete version of Noether's conservation theorem.

5.2. Variational Lie group integrator for the impact of a beam

The integrator is obtained, as in the previous example, by considering the discrete nonsmooth field theoretic setting developed in Section 3, with the configuration space $\mathcal{C}_d^{\mathbf{I}}$.

In order to preserve the Lie group description of this problem at the discrete level, we follow the approach developed in [3] and [32] for field theoretic (multisymplectic) Lie group integrators. These integrators adapt to the field theoretic setting the variational integrators on Lie groups developed in [48].

This approach involves the choice of a *retraction map* $\tau : \mathfrak{g} \to G$ to consistently encode in the Lie algebra the discrete displacement made on the Lie group. By definition, a *retraction map* is a diffeomorphism around the origin such that $\tau(0) = e$, the identity element in G, and the derivative of τ at e is the identity map.

Consequently, the discrete velocities and strains ξ_a^j and η_a^j are defined from the values $g_a^j = (\Lambda_a^j, \mathbf{r}_a^j) \in G := SE(3)$ of the discrete field, through a retraction map $\tau : \mathfrak{g} \to G$ by

$$\begin{aligned} \xi_a^j &:= \tau^{-1}\left((g_a^j)^{-1} g_a^{j+1}\right)/\Delta t^j \in \mathfrak{g}, \quad \text{with } \Delta t^j := t^{j+1} - t^j, \\ \eta_a^j &:= \tau^{-1}\left((g_a^j)^{-1} g_{a+1}^j\right)/\Delta s_a \in \mathfrak{g}, \quad \text{with } \Delta s_a := s_{a+1} - s_a. \end{aligned} \tag{5.8}$$

The Lagrangian (5.1) is approximated on the rectangle $\square_a^j$ as

$$\begin{aligned} \mathcal{L}_a^j &= \mathcal{L}_d(\square_a^j, g_a^j, g_a^{j+1}, g_{a+1}^j, g_{a+1}^{j+1}, \xi_a^j, \xi_{a+1}^j, \eta_a^j, \eta_a^{j+1}) \\ &= \frac{1}{2}\Delta s \Delta t^j \Big[\frac{1}{2}\langle \mathbb{J}\xi_a^j, \xi_a^j\rangle + \frac{1}{2}\langle \mathbb{J}\xi_{a+1}^j, \xi_{a+1}^j\rangle - \frac{1}{2}\langle \mathbb{C}\,(\eta_a^j - \mathbf{E}_6), (\eta_a^j - \mathbf{E}_6)\rangle \\ &\quad - \frac{1}{2}\langle \mathbb{C}\,(\eta_a^{j+1} - \mathbf{E}_6), (\eta_a^{j+1} - \mathbf{E}_6)\rangle - \Pi_d(g_a^j)\Big], \end{aligned} \tag{5.9}$$

where the discrete potential energy Π_d is defined as the gravitational potential energy density

$$\Pi_d(g_a^j, g_a^{j+1}, g_{a+1}^j, g_{a+1}^{j+1}) := \frac{1}{4}\left(\left\langle \mathbf{q}_a, g_a^j\right\rangle + \left\langle \mathbf{q}_a, g_a^{j+1}\right\rangle + \left\langle \mathbf{q}_{a+1}, g_{a+1}^j\right\rangle + \left\langle \mathbf{q}_{a+1}, g_{a+1}^{j+1}\right\rangle\right),$$

where $\mathbf{q} = \Delta g \rho a^2 \mathbf{E}_3$, for the beam with given square cross-section $\mathcal{S}$ of side a, material density ρ, distance between two nodes in the reference configuration Δs, and gravitational acceleration vector $g\mathbf{E}_3$. The impenetrability condition $\psi : SE(3) \to \mathbb{R}$ is given by (5.6).

Contrary to the previous example, the contact can arise at any node and there are several contact times. The discrete base space configuration ϕ_{X_d} thus assigns to the indices $\tilde{\imath}_1, \ldots, \tilde{\imath}_K$ the times of contact $\widetilde{t}_1, \ldots, \widetilde{t}_K$, thereby generalizing (3.3) to the case of several contact times. To each of these times is associated a discrete domain D_d (see Def. (3.6)). Below, we present the discrete algorithm for one contact time; the generalization to several contact times is obvious. We use the notation defined in (4.4) for the time steps Δt and $\Delta\widetilde{t}$.

We derive our numerical scheme by applying Theorem 3.1. The discrete equations follow from tedious computations that we summarize in Appendix A. They depend on the momenta μ_a^j and λ_a^j defined by

$$\mu_a^j := \left(\mathrm{d}\tau^{-1}_{\Delta t \xi_a^j}\right)^* \frac{\partial K}{\partial \xi}\left(\xi_a^j\right) \quad \text{and} \quad \lambda_a^j := \left(\mathrm{d}\tau^{-1}_{\Delta s \eta_a^j}\right)^* \frac{\partial \Phi}{\partial \eta}\left(\eta_a^j\right), \tag{5.10}$$

with the help of the right trivialized derivative $\mathrm{d}^R\tau_\xi^{-1}$ of the inverse of the retraction map (see Appendix A). We use below the expression of the adjoint and coadjoint operators of $SE(3)$, given by

$$\begin{aligned} \mathrm{Ad}_{(\Lambda,\mathbf{r})}(\boldsymbol{\omega}, \boldsymbol{\gamma}) &:= (\Lambda\boldsymbol{\omega}, \Lambda\boldsymbol{\gamma} + \mathbf{r} \times \Lambda\boldsymbol{\omega}) \\ \mathrm{Ad}^*_{(\Lambda,\mathbf{r})}(\boldsymbol{\mu}, \boldsymbol{\nu}) &:= (\Lambda^T(\boldsymbol{\mu} + \boldsymbol{\nu} \times \mathbf{r}), \Lambda^T\boldsymbol{\gamma}). \end{aligned} \tag{5.11}$$

(i) Away from the contact time, i.e., for $j \in \{1, \ldots, i-1\} \cup \{i, \ldots, N-1\}$, we have:

(a) The DEL field equations for all $a = 1, \ldots, A-1$:

$$\begin{aligned} &2\Delta s(-\mu_a^j + \mathrm{Ad}^*_{\tau(\Delta t^{j-1}\xi_a^{j-1})}\mu_a^{j-1}) + (\Delta t^j + \Delta t^{j-1})(\lambda_a^j - \mathrm{Ad}^*_{\tau(\Delta s \eta_{a-1}^j)}\lambda_{a-1}^j) \\ &\quad = \Delta s(\Delta t^j + \Delta t^{j-1})(g_a^j)^{-1}\mathbf{q}_a. \end{aligned}$$

(b) The two equations for zero traction boundary conditions at $a = 0$ and $a = A$:

$$\begin{cases} \Delta s\left(-\mu_0^j + \mathrm{Ad}^*_{\tau(\Delta t^{j-1}\xi_0^{j-1})}\mu_0^{j-1}\right) + (\Delta t^{j-1} + \Delta t^j)\lambda_0^j \\ \quad = \dfrac{1}{2}\Delta s(\Delta t^{j-1} + \Delta t^j)(g_0^j)^{-1}\mathbf{q}_0, \\ \Delta s\left(-\mu_A^j + \mathrm{Ad}^*_{\tau(\Delta t^{j-1}\xi_A^{j-1})}\mu_A^{j-1}\right) - (\Delta t^{j-1} + \Delta t^j)\mathrm{Ad}^*_{\tau(\Delta s \eta_{A-1}^j)}\lambda_{A-1}^j \\ \quad = \dfrac{1}{2}\Delta s(\Delta t^{j-1} + \Delta t^j)(g_A^j)^{-1}\mathbf{q}_A. \end{cases}$$

(ii) At the impact time $\widetilde{t}$, for all $a \in \{1, \dots, A-1\}$, the position g_a^i at time t^i and the Lagrangian multiplier $\mathbb{\lambda}_a < 0$ are obtained by solving the system including the following terms:

(a) energy conservation during the impact (horizontal discrete jump condition):

$$\sum_{a=0}^{A-1} \widetilde{E}_a = \sum_{a=0}^{A-1} E_a^{i-1};$$

(b) if the contact happens at an interior node, the discrete jump condition involving Lagrange multipliers:

$$\begin{aligned} &2\Delta s(-\widetilde{\mu}_a + \mathrm{Ad}^*_{\tau(\Delta t^{i-1}\xi_a^{i-1})}\mu_a^{i-1}) + (\Delta t^{i-1} + \Delta\widetilde{t})(\widetilde{\lambda}_a - \mathrm{Ad}^*_{\tau(\Delta s\widetilde{\eta}_{a-1})}\widetilde{\lambda}_{a-1}) \\ &\quad = \Delta s(\Delta t^{i-1} + \Delta\widetilde{t})(\widetilde{g}_a)^{-1}\mathbf{q}_a + 2\widetilde{\mathbb{\lambda}}_a(\widetilde{g}_a)^{-1}D_g\psi(\widetilde{g}_a); \end{aligned}$$

(c) if the contact happens at an extremity ($a = 0$ or $a = A$), the two equations for zero traction boundary conditions:

$$\begin{cases} \Delta s\left(-\widetilde{\mu}_0 + \mathrm{Ad}^*_{\tau(\Delta t^{i-1}\xi_0^{i-1})}\mu_0^{i-1}\right) + (\Delta t^{i-1} + \Delta\widetilde{t})\widetilde{\lambda}_0 \\ \quad = \dfrac{1}{2}\Delta s(\Delta t^{i-1} + \Delta\widetilde{t})(\widetilde{g}_0)^{-1}\mathbf{q}_0 + \widetilde{\mathbb{\lambda}}_0(\widetilde{g}_0)^{-1}D_g\psi(\widetilde{g}_0), \\ \Delta s\left(-\widetilde{\mu}_A + \mathrm{Ad}^*_{\tau(\Delta t^{i-1}\xi_A^{i-1})}\mu_A^{i-1}\right) - (\Delta t^{i-1} + \Delta\widetilde{t})\mathrm{Ad}^*_{\tau(\Delta s\widetilde{\eta}_{A-1})}\widetilde{\lambda}_{A-1} \\ \quad = \dfrac{1}{2}\Delta s(\Delta t^{i-1} + \Delta\widetilde{t})(\widetilde{g}_A)^{-1}\mathbf{q}_A + \widetilde{\mathbb{\lambda}}_A(\widetilde{g}_A)^{-1}D_g\psi(\widetilde{g}_A), \end{cases}$$

where $(\widetilde{g}_a)^{-1}D_g\psi(\widetilde{g}_a) = (0, \widetilde{\Lambda}_a^T\mathbf{E}_3)$. Accordingly, the contact force, normal to the plate, is given by

$$\mathbf{f}_{cont} := \widetilde{\mathbb{\lambda}}_a D_g\psi(\widetilde{g}_a) = \widetilde{\mathbb{\lambda}}_a(0, \mathbf{E}_3)^T.$$

Discrete Noether's Theorem. The discrete Lagrangian (5.9) has the same symmetry invariance properties as its continuous counterpart (5.1), namely, it is invariant with respect to the subgroup of $SE(3)$ defined by translations that are parallel to the plane $z_3 = 0$ and by rotations around the vertical axis. Applying the discrete Noether theorem, as expressed in (3.15), we get the discrete conservation law

$$\begin{aligned} \mathbf{J}(\mathbf{g}^j, \boldsymbol{\xi}^j) &:= \left\langle \sum_{a=0}^{A-1} \left[\frac{\Delta s}{2}\left(\mathrm{Ad}^*_{(g_a^j)^{-1}}\mu_a^j + \mathrm{Ad}^*_{(g_{a+1}^j)^{-1}}\mu_{a+1}^j\right) - \frac{\Delta t^j \Delta s}{4}(\mathbf{q}_a + \mathbf{q}_{a+1})\right], (0,0,1,1,1,0)^T \right\rangle \\ &= constant, \end{aligned}$$

where $\mathbf{g}^j := (g_0^j, \dots, g_A^j)$, $\boldsymbol{\xi}^j := (\xi_0^j, \dots, \xi_A^j)$.

5.3. Numerical tests

We consider the collision of the beam on a plane, for various discretization rates Δs and Δt, and different speeds of impact from ≈30 to ≈6 m/s. The algorithm used in the test is the one described in Section 4.3.1, i.e., the *contact time integrator 1*, which is easy to understand and to implement. Moreover, it is related to Theorem 3.1 in an obvious way. (In a forthcoming paper we will use the *contact time integrator 2* in order to study the contact of nonlinear elastic models.)

5.3.1. Short time evolution $T = 0.5$ s for high velocity impact

Initial conditions. We consider the initial value problem of a geometrically exact beam with length $L = 0.5$ m and square cross-section $\mathcal{S}$ of side $a = 0.05$ m, so $|\mathcal{S}| = a^2$ and $I_1 = I_2 = \rho\frac{a^4}{12}$. The beam parameters are $\rho = 10^3$ kg/m^3, $E = 10^3$ N/m^2, $\nu = 0.35$. The gravitational acceleration is taken to be g = 10 m/s^2. The initial conditions are given by the configuration $g_a^0 = (\Lambda_a^0, \mathbf{r}_a^0)$ and the initial velocity $\xi_a^0 = (\boldsymbol{\omega}_a^0, \boldsymbol{\gamma}_a^0)$ at time $t = t^0$ for all nodes $a = 0, \dots, A$.

We choose

$$g_0^0 = \left(\begin{bmatrix} 1 & 0 & 0 \\ 0 & \cos(0.5) & -\sin(0.5) \\ 0 & \sin(0.5) & \cos(0.5) \end{bmatrix}, \begin{bmatrix} 0 \\ 0 \\ 0 \end{bmatrix} \right), \quad g_{a+1}^0 = g_a^0\, \tau(\Delta s\, \eta_a^0), \quad \text{for all } a = 0, \dots, A-1,$$

where $\eta_a^0 = (1, 4.5, 1, 0, 0, 1)$, for all $a = 0, \dots, A-1$, and

$$g_0^1 = \left(\begin{bmatrix} 1 & 0 & 0 \\ 0 & \cos(0.5) & -\sin(0.5) \\ 0 & \sin(0.5) & \cos(0.5) \end{bmatrix}, \begin{bmatrix} 0 \\ -2 \cdot 10^{-5}\sin(0.5) \\ 2 \cdot 10^{-5}\cos(0.5) \end{bmatrix} \right), \quad g_{a+1}^1 = g_a^1\, \tau(\Delta s\, \eta_a^1), \tag{5.12}$$

$$\text{for all } a = 0, \dots, A-1, \quad \text{where } \eta_a^1 = (1.004, 4.522, 0.996, -0.004, 0, 1). \tag{5.13}$$

The initial velocity is given by

$$\xi_a^0 = \frac{1}{(4 \cdot 10^{-5})} \tau^{-1}((g_a^0)^{-1} g_a^1), \quad \text{for all } a = 0, \dots, A. \tag{5.14}$$

We now add the plane $z^3 = 0$ as an obstacle for the beam.

Robustness to space–time discretization. We observe in Fig. 5.1 that our approach is robust to spatial and temporal discretization since the behavior of the beam remains coherent for various sizes of Δs and Δt. We estimate the speed of the first impact, due to the chosen initial conditions (5.12), to be about 30 m/s.

Energy and momentum maps. We observe excellent conservation of both the energy and the angular and linear momenta associated to the invariance of the mechanical system with respect to translations parallel to the plane $z^3 = 0$, and to rotations around the vertical axis, see Fig. 5.2.

5.3.2. *Time evolution $T = 2.5$ s for a reduced impact speed*

The initial conditions (5.12) are modified. The speed ξ_a^0, in each node and at time t^0, is reduced such that

$$\xi_a^0 = \frac{1}{(8 \cdot 10^{-5})} \tau^{-1}((g_a^0)^{-1} g_a^1), \quad \text{for all } a = 0, \dots, A. \tag{5.15}$$

As a consequence, the speed at the first impact is reduced to about 15 m/s. The duration of the test is 2.5 s, that is five times the previous one; the general motion of the beam is unchanged.

In Fig. 5.3, we observe a good conservation of the linear momentum map and of the energy. However, the angular momentum map $\mathbf{J}_1$ fails to be exactly conserved, showing a slight decay after approximately 1 s of simulation. The reason for this is that, at the time of contact $\widetilde{t}$, we have to calculate the value of the Lagrange multiplier $\widetilde{\lambda}$ by minimizing a function while enforcing energy conservation (the horizontal jump condition). When the impact is very weak (close to sliding), we have to find the global minimum for a nonlinear problem among a large amount of local minima. It therefore becomes very difficult to get a good numerical approximation of the right solution, even if we reduce the time step: it can happen that we are not exactly in contact and yet, within the tolerance of the gap function.

5.3.3. *Longer-time evolution $T = 5$ s for moderate impact*

The initial conditions (5.12) are modified in order to get a speed estimated to about 6 m/s at the first impact. The value of ξ_a^0 is now

$$\xi_a^0 = \frac{1}{(20 \cdot 10^{-5})} \tau^{-1}((g_a^0)^{-1} g_a^1), \quad \text{for all } a = 0, \dots, A. \tag{5.16}$$

Note that at such a reduced impact speed, the value of the Lagrangian multiplier λ is close to zero, which triggers added iterations during the numerical minimization algorithm to get the required accuracy. In addition, the intensity of the reaction force being low, the beam stays in contact during a long time: the bar, composed of 10 elements, undergoes ≈200 contacts. Despite these difficult conditions, the energy is well conserved over a time interval of 5 s. The results of the simulations for two different time-steps are given in Fig. 5.4.

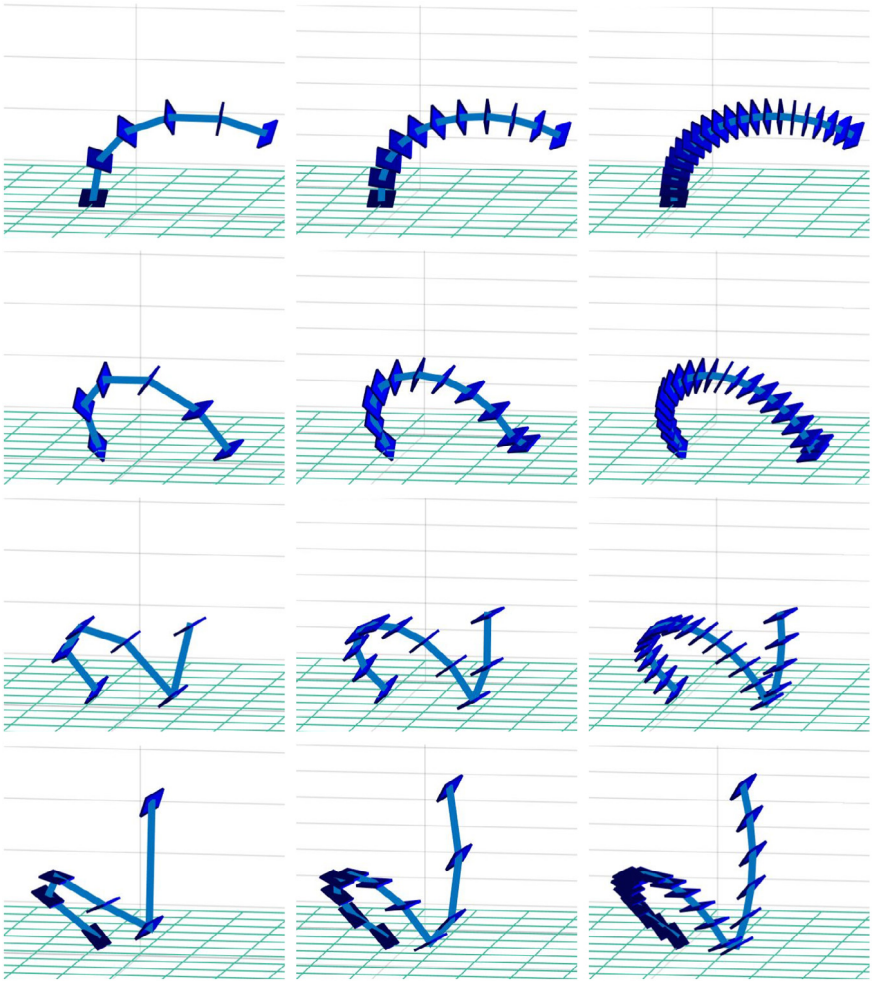

Fig. 5.1. Beam with frictionless collision on a plane. From left to right: beam composed of 5 elements with $\Delta t = 0.00004$ s, composed of 10 elements with $\Delta t = 0.00004$ s, and composed of 20 elements with $\Delta t = 0.00001$ s. From top to the bottom : at times $t = 0$ s, $t = 0.0053$ s, $t = 0.01$ s, $t = 0.015$ s.

6. Conclusions

We have presented in this paper a new approach to simulate dynamic contact problems that provides a rigorous geometric discretization of the continuous theory. The main interest of our proposed multisymplectic time stepping approach is justified by Theorem 3.1 which allows to get a discrete trajectory during contact that conserves energy and most of the symmetries, without having recourse to any additional ad hoc treatment of the contact release. Moreover, we pointed out that the way a contact problem is spatially discretized can be crucial if one wants to mimic perfectly the physical behavior of a contact, see Fig. 4.3 compared to Fig. 4.2. While we presented only two 1D dynamical systems, we believe that the results generated by our approach makes multisymplecticity a credible tool to handle contacts as these 1D problems are notoriously difficult to handle numerically with current integrators.

The next step of this research will try to better preserve angular momenta when we study the impact of a nonlinear elastic model against a smooth surface over a long period of time. Other avenues of investigation include the treatment of contact for 2D and 3D objects.

Acknowledgments

We are very grateful to Alain Curnier for his constant advice and interest in our results during the elaboration of this work. We are indebted to Lyudmila Grigoryeva for many helpful discussions.

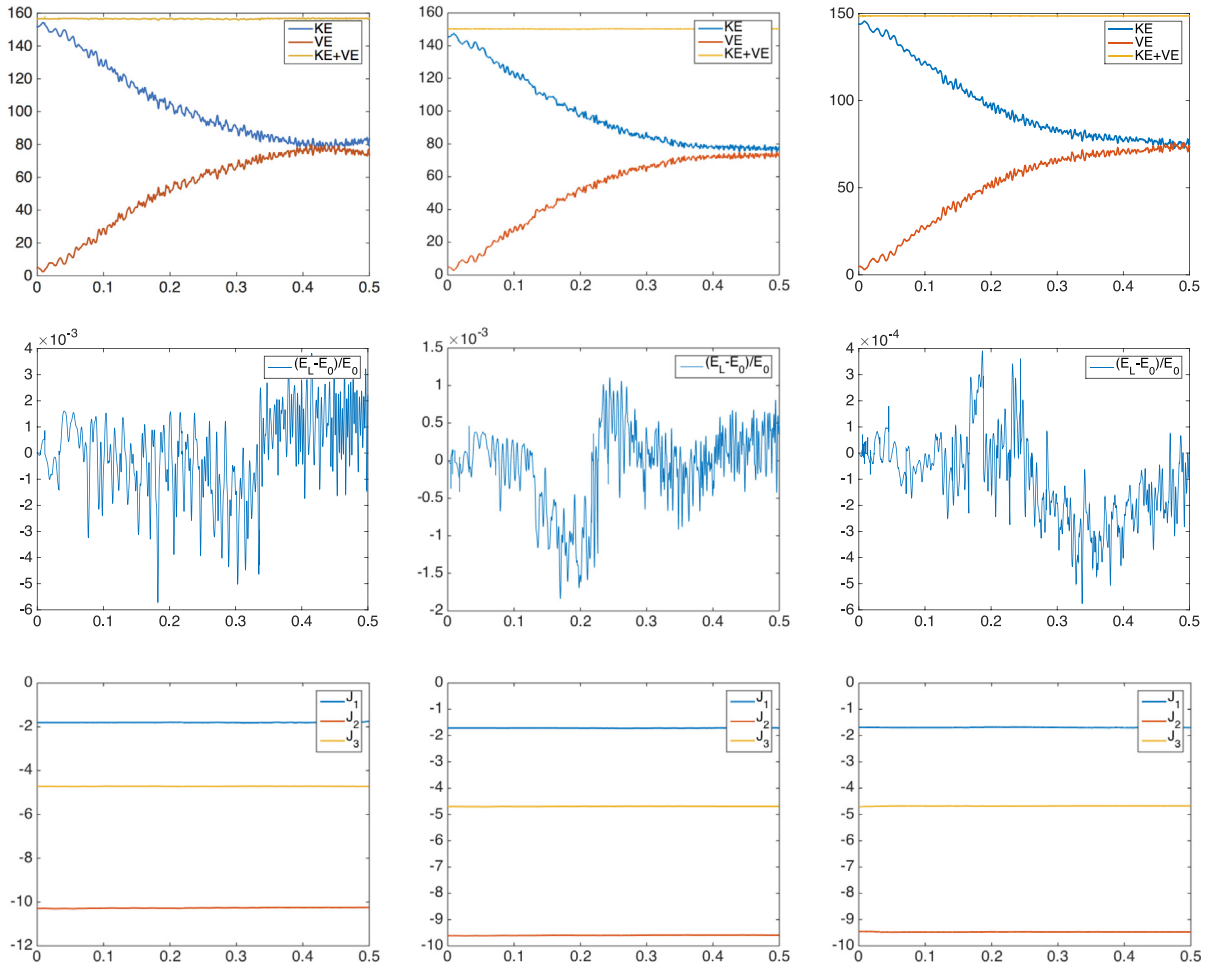

Fig. 5.2. Beam with collision on a plane. From top to bottom: Total energy, relative error, angular and linear momentum. From left to right: beam composed of 5 elements with $\Delta t = 0.00004$ s, composed of 10 elements with $\Delta t = 0.00004$ s, and composed of 20 elements with $\Delta t = 0.00001$ s. Interval of time [0, 0.5].

The first author was partially supported by the European Research Council Advanced Grant 267382 FCCA. The first and second authors were partially supported by the ANR project GEOMFLUID, ANR-14-CE23-0002-01. The third author was partially supported by NSF grant CCF-1011944. The fourth author were partially supported by the Swiss National Science Foundation grant NCCR SwissMAP.

Appendix A. Discrete field theoretic Hamilton's principle

In this appendix, we briefly review the derivation of the DEL equations and zero traction boundary conditions from the discrete field theoretic Hamilton principle. Since we focus exclusively on the DEL field equations, we assume that we only need to consider vertical variations: it is enough to consider the discrete field $\varphi_d : U_{X_d} \to M$ denoted as $g_d : U_{X_d} \to SE(3)$ in this case. The horizontal variations can be incorporated easily by using the general approach described in Section 3.1.

The discrete action functional is $\mathfrak{S}_d^{ns}(g_d) = \sum_{a=0}^{A-1} \sum_{j=0}^{N-1} \mathcal{L}_a^j$, where we recall that

$$\mathcal{L}_a^j := \mathcal{L}_d(\square_a^j, g_a^j, g_a^{j+1}, g_{a+1}^j, g_{a+1}^{j+1}, \xi_a^j, \xi_{a+1}^j, \eta_a^j, \eta_a^{j+1}).$$

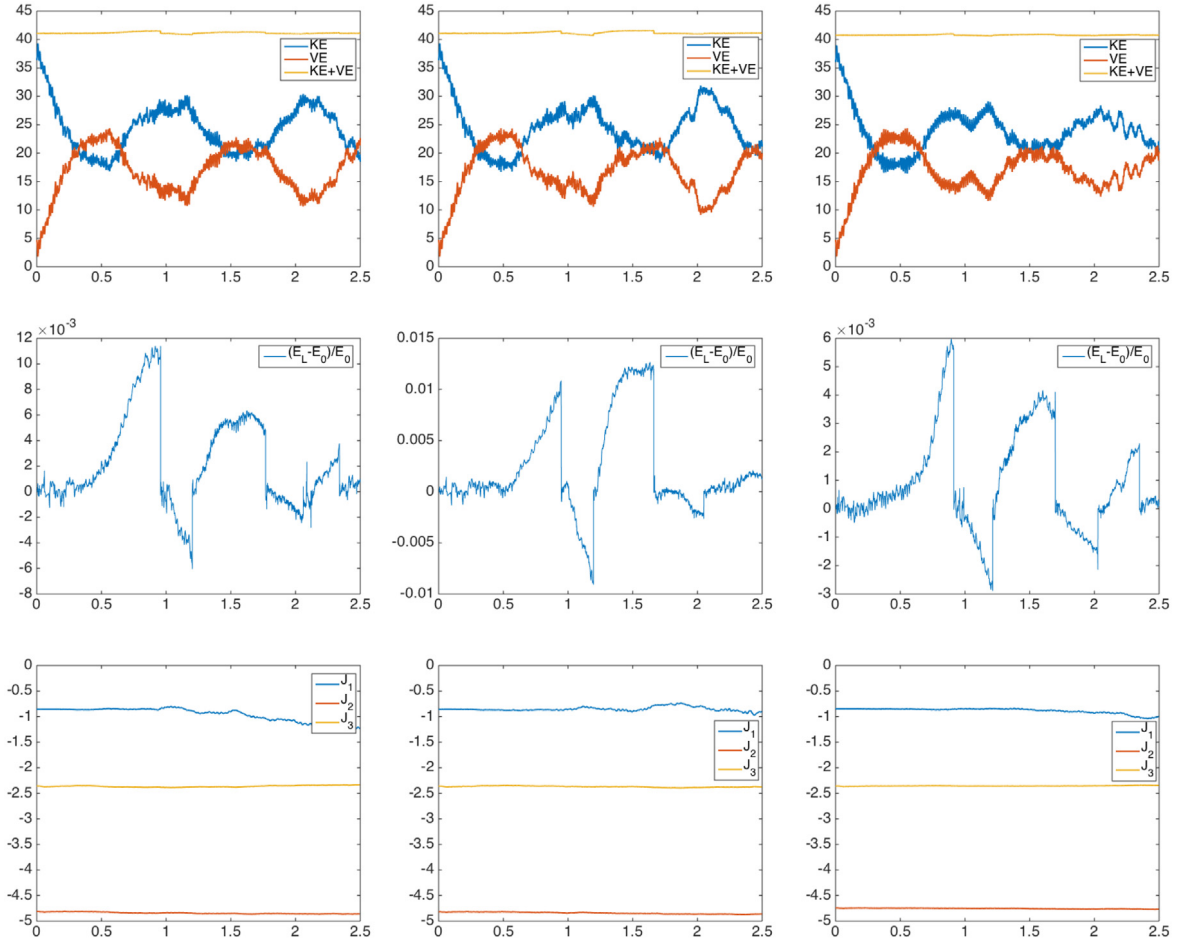

Fig. 5.3. Impacts of a beam on a plane during 2.5 s. From top to bottom: Total energy, relative error, angular and linear momentum. From left to right: (1) beam composed of 10 elements with $\Delta t = 0.00004$ s, (2) beam composed of 10 elements with $\Delta t = 0.00002$ s, (3) beam composed of 16 elements with $\Delta t = 0.00002$ s.

To compute the variation $\delta \mathfrak{S}_d(g_d)$, we need the expressions of the variations $\delta \xi_a^j$ and $\delta \eta_a^j$ induced by variations of g_d. Using the definition of ξ_a^j and η_a^j in terms of g_a^j given in (5.8), we obtain the constrained variations

$$\begin{aligned} \delta \xi_a^j &= \mathrm{d}^R \tau^{-1}_{\Delta t \xi_a^j} \left(-\zeta_a^j + \mathrm{Ad}_{\tau(\Delta t \xi_a^j)} \zeta_a^{j+1} \right) / \Delta t, \\ \delta \eta_a^j &= \mathrm{d}^R \tau^{-1}_{\Delta s \eta_a^j} \left(-\zeta_a^j + \mathrm{Ad}_{\tau(\Delta s \eta_a^j)} \zeta_{a+1}^j \right) / \Delta s, \end{aligned} \tag{A.1}$$

where $\zeta_a^j = (g_a^j)^{-1} \delta g_a^j$ can be arbitrarily chosen in $\mathfrak{se}(3)$; see, e.g., [49] for a derivation of such expressions. In these expressions, $\mathrm{d}^R \tau_\xi^{-1}$ denotes the right trivialized derivative of τ^{-1}, defined by

$$\mathrm{d}^R \tau_\xi^{-1} : \mathfrak{g} \to \mathfrak{g}, \quad \mathrm{d}^R \tau_\xi^{-1}(\eta) := D\tau^{-1}(g) \cdot (\eta g),$$

where $g := \tau(\xi) \in SE(3)$ and $D\tau^{-1}(g) \cdot (\eta g)$ denotes the derivative of τ^{-1} at the Lie group element g, in the direction ηg (cf. [48]). The retraction map $\tau : \mathfrak{se}(3) \to SE(3)$ is chosen to be the Cayley map [3] since it is numerically more efficient than the exponential map (see, e.g., [3,30]).

[3] If we embed the special Euclidean group $SE(3) \subset SL(4, \mathbb{R})$ and its Lie algebra $\mathfrak{se}(3) \subset \mathfrak{sl}(4, \mathbb{R})$ by

$$SE(3) \ni (\Lambda, \mathbf{r}) \mapsto \begin{bmatrix} \Lambda & \mathbf{r} \\ \mathbf{0}^T & 1 \end{bmatrix} \in SL(4, \mathbb{R}), \qquad \mathfrak{se}(3) \ni (\omega, \boldsymbol{\gamma}) \mapsto \begin{bmatrix} \omega & \boldsymbol{\gamma} \\ \mathbf{0}^T & 0 \end{bmatrix} \in \mathfrak{sl}(4, \mathbb{R}).$$

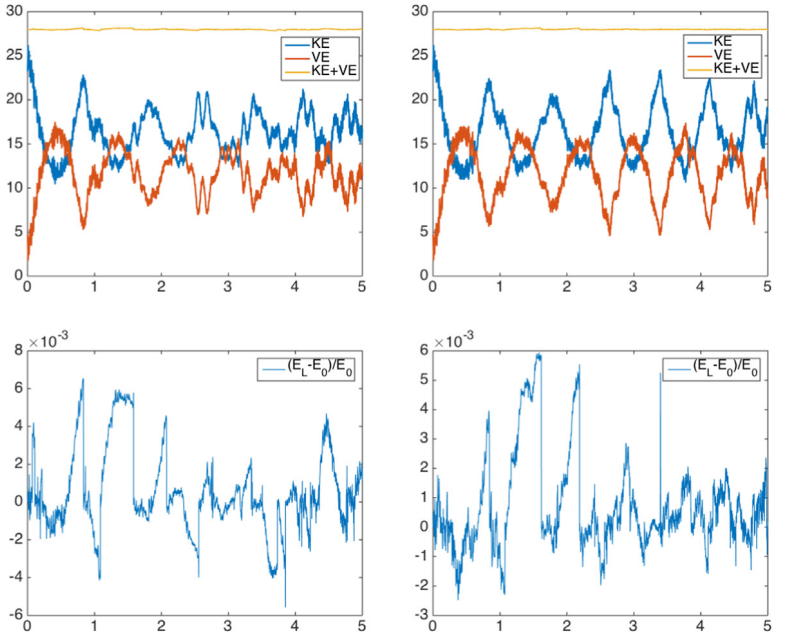

Fig. 5.4. Impacts of a beam on a plane during 5 s. From top to bottom: Total energy, and relative error. From left to right: (1) beam composed of 10 elements with $\Delta t = 0.00004$ s, and number of contacts ≈200, (2) beam composed of 10 elements with $\Delta t = 0.00002$ s, and number of contacts ≈200.

Taking the variations of $\mathfrak{S}_d^{ns}(g_d)$, using the specific form (A.1) for $\delta\xi_a^j$ and $\delta\eta_a^j$, and collecting the terms proportional to ζ_a^j, we get the expression

$$\begin{aligned}
\delta\mathfrak{S}_d(g_d) &= \frac{1}{2}\sum_{j=0}^{N-1}\sum_{a=0}^{A-1}\left\{\mathbb{A}_a^j\cdot\zeta_a^j + \mathbb{B}_a^j\cdot\zeta_a^{j+1} + \mathbb{C}_a^j\cdot\zeta_{a+1}^j + \mathbb{D}_a^j\cdot\zeta_{a+1}^{j+1}\right\}\\
&= \frac{1}{2}\sum_{j=1}^{N-1}\sum_{a=1}^{A-1}\left(\mathbb{A}_a^j + \mathbb{B}_a^{j-1} + \mathbb{C}_{a-1}^j + \mathbb{D}_{a-1}^{j-1}\right)\cdot\zeta_a^j\\
&\quad + \frac{1}{2}\sum_{a=1}^{A-1}\left(\left(\mathbb{A}_a^0 + \mathbb{C}_{a-1}^0\right)\cdot\zeta_a^0 + \left(\mathbb{B}_a^{N-1} + \mathbb{D}_{a-1}^{N-1}\right)\cdot\zeta_a^N\right)\\
&\quad + \frac{1}{2}\sum_{j=1}^{N-1}\left(\left(\mathbb{A}_0^j + \mathbb{B}_0^{j-1}\right)\cdot\zeta_0^j + \left(\mathbb{C}_{A-1}^j + \mathbb{D}_{A-1}^{j-1}\right)\cdot\zeta_A^j\right)\\
&\quad + \frac{1}{2}\left(\mathbb{A}_0^0\cdot\zeta_0^0 + \mathbb{B}_0^{N-1}\cdot\zeta_0^N + \mathbb{C}_{A-1}^0\cdot\zeta_A^0 + \mathbb{D}_{A-1}^{N-1}\cdot\zeta_A^N\right),
\end{aligned} \tag{A.2}$$

where

$$\mathbb{A}_a^j = -\Delta s\mu_a^j + \Delta t^j\lambda_a^j - \frac{1}{2}\Delta s\Delta t^j(g_a^j)^{-1}D_{g_a^j}\Pi_d(g_a^j),$$

$$\mathbb{B}_a^j = \Delta s\mathrm{Ad}^*_{\tau(\Delta t^j\xi_a^j)}\mu_a^j + \Delta t^j\lambda_a^{j+1} - \frac{1}{2}\Delta s\Delta t^j(g_a^{j+1})^{-1}D_{g_a^{j+1}}\Pi_d(g_a^{j+1}),$$

The usual way to define a Cayley map for $SE(3)$ is to define the map $\tau : \mathfrak{se}(3) \to SE(3)$ by

$$\begin{aligned}
\tau(\omega,\boldsymbol{\gamma}) &:= \left(\mathbf{I}_4 - \frac{1}{2}\begin{bmatrix}\omega & \boldsymbol{\gamma}\\ \mathbf{0}^T & 0\end{bmatrix}\right)^{-1}\left(\mathbf{I}_4 + \frac{1}{2}\begin{bmatrix}\omega & \boldsymbol{\gamma}\\ \mathbf{0}^T & 0\end{bmatrix}\right)\\
&= \begin{bmatrix}\left(\mathbf{I}_3 - \frac{\omega}{2}\right)^{-1}\left(\mathbf{I}_3 + \frac{\omega}{2}\right) & \frac{4}{4+\|\boldsymbol{\omega}\|^2}\left(\mathbf{I}_3 + \frac{1}{2}\omega + \frac{1}{4}\boldsymbol{\omega}\boldsymbol{\omega}^T\right)\boldsymbol{\gamma}\\ \mathbf{0}^T & 1\end{bmatrix}.
\end{aligned}$$

$$\mathbb{C}_a^j = -\Delta s \mu_{a+1}^j - \Delta t^j \mathrm{Ad}^*_{\tau(\Delta s \eta_a^j)} \lambda_a^j - \frac{1}{2}\Delta s \Delta t^j (g_{a+1}^j)^{-1} D_{g_{a+1}^j} \Pi_d(g_{a+1}^j),$$

$$\mathbb{D}_a^j = \Delta s \mathrm{Ad}^*_{\tau(\Delta t^j \xi_{a+1}^j)} \mu_{a+1}^j - \Delta t^j \mathrm{Ad}^*_{\tau(\Delta s \eta_a^{j+1})} \lambda_a^{j+1} - \frac{1}{2}\Delta s \Delta t^j (g_{a+1}^{j+1})^{-1} D_{g_{a+1}^{j+1}} \Pi_d(g_{a+1}^{j+1}).$$

Recall that μ_a^j and λ_a^j are the momenta defined in (5.10) and Ad^* is the coadjoint action of $SE(3)$ defined in (5.11).

DEL field equations on Lie groups. They are obtained by requiring stationarity of the action functional with respect to field variations at the interior nodes. From (A.2), we thus get

$$\begin{aligned} &2\Delta s(-\mu_a^j + \mathrm{Ad}^*_{\tau(\Delta t^{j-1}\xi_a^{j-1})}\mu_a^{j-1}) + (\Delta t^j + \Delta t^{j-1})(\lambda_a^j - \mathrm{Ad}^*_{\tau(\Delta s \eta_{a-1}^j)}\lambda_{a-1}^j) \\ &\quad -\Delta s(\Delta t^j + \Delta t^{j-1})(g_a^j)^{-1} D_{g_a^j}\Pi_d(g_a^j) = 0, \\ &\quad \text{for all } j \in \{1, \dots, N-1\} \text{ and } a \in \{1, \dots, A-1\}. \end{aligned} \tag{A.3}$$

Discrete zero traction boundary conditions. They are obtained, exactly as in the continuous case, by considering variations of the field values at the boundaries $a = 0$ and $a = A$. This yields the two equations

$$\begin{aligned} &\Delta s\left(-\mu_0^j + \mathrm{Ad}^*_{\tau(\Delta t^{j-1}\xi_0^{j-1})}\mu_0^{j-1}\right) + (\Delta t^{j-1} + \Delta t^j)\lambda_0^j \\ &\quad -\frac{1}{2}\Delta s(\Delta t^{j-1} + \Delta t^j)(g_0^j)^{-1} D_{g_0^j}\Pi_d(g_0^j) = 0, \\ &\Delta s\left(-\mu_A^j + \mathrm{Ad}^*_{\tau(\Delta t^{j-1}\xi_A^{j-1})}\mu_A^{j-1}\right) - (\Delta t^{j-1} + \Delta t^j)\mathrm{Ad}^*_{\tau(\Delta s \eta_{A-1}^j)}\lambda_{A-1}^j \\ &\quad -\frac{1}{2}\Delta s(\Delta t^{j-1} + \Delta t^j)(g_A^j)^{-1} D_{g_A^j}\Pi_d(g_A^j) = 0, \\ &\forall j \in \{1, \dots, N-1\}. \end{aligned} \tag{A.4}$$

We refer to [3] for a complete treatment of boundary conditions in the discrete field theoretic context.

References

[1] A. Pandolfi, C. Kane, J.E. Marsden, M. Ortiz, Time-discretized variational formulation of non-smooth frictional contact, Internat. J. Numer. Methods Engrg. 53 (2002) 1801–1829.

[2] A. Lew, J.E. Marsden, M. Ortiz, M. West, Asynchronous variational integrators, Arch. Ration. Mech. Anal. 167 (2) (2003) 85–146.

[3] F. Demoures, F. Gay-Balmaz, T.S. Ratiu, Multisymplectic variational integrator and space/time symplecticity, Anal. Appl. 14 (3) (2014) 341–391. http://arxiv.org/pdf/1310.4772.pdf.

[4] A. Curnier, Unilateral contact, mechanical modeling, in: New Developments in Contact Problems, in: P. Wriggers, P. Panagiotopoulos (Eds.), CISM Courses and Lectures, vol. 388, International Center for Mechanical Sciences, Springer-Verlag, Wien, 1999, pp. 1–54.

[5] F.H. Clarke, Optimization and Nonsmooth Analysis, in: Classics in Applied Mathematics, vol. 5, SIAM, Philadelphia, PA, 1990.

[6] J.-J. Moreau, Fonctions convexes duales et points proximaux dans un espace hilbertien, C. R. Acad. Sci. Paris 255 (1962) 2897–2899.

[7] J.-J. Moreau, Théorèmes inf-sup, C. R. Acad. Sci. Paris 258 (1964) 2720–2722.

[8] J.-J. Moreau, Fonctionnelles convexes. SéMinaire Sur Les éQuations Aux dérivéEs Partielles, Collège de France, 1966.

[9] R.T. Rockafellar, Convex Functions and Dual Extremum Problems (Ph.D. thesis), Harvard University, Cambridge, Massachusetts, 1963.

[10] R.T. Rockafellar, Characterization of the subdifferentials of convex functions, Pacific J. Math. 17 (1966) 497–510.

[11] A. Curnier, An augmented Lagrangian method for discrete large-slip contact problems, Internat. J. Numer. Methods Engrg. 36 (1993) 569–593.

[12] T. Laursen, V. Chawla, Design of energy conserving algorithms for frictionless dynamic contact problems, Internat. J. Numer. Methods Engrg. 40 (5) (1997) 863–886.

[13] F. Armero, E. Petocz, Formulation and analysis of conserving algorithms for frictionless dynamic contact/impact problems, Comput. Methods Appl. Mech. Engrg. 158 (3–4) (1998) 269–300.

[14] C. Kane, E.A. Repetto, M. Ortiz, J.E. Marsden, Finite element analysis of nonsmooth contact, Comput. Methods Appl. Mech. Engrg. 180 (1999) 1–26.

[15] P. Wriggers, Computational Contact Mechanics, Wiley, 2002.

[16] T. Laursen, Computational Contact and Impact Mechanics, Springer-Verlag, 2002.

[17] T. Laursen, G. Love, Improved implicit integrators for transient impact problems; dynamic frictional dissipation within an admissible conserving framework, Comput. Methods Appl. Mech. Engrg. 192 (19) (2003) 2223–2248.

[18] F. Cirak, M. West, Decomposition contact response (DCR) for explicit finite element dynamics, Internat. J. Numer. Methods Engrg. 64 (2005) 1078–1110.

[19] P. Wriggers, T.A. Laursen, Computational Contact Mechanics, in: CISM Courses and Lectures, vol. 298, Springer-Verlag, 2007.

[20] G. Johnson, S. Leyendecker, M. Ortiz, Discontinuous variational time integrators for complex multibody collisions, Internat. J. Numer. Methods Engrg. 100 (2014) 871–913.
[21] F. Demoures, F. Gay-Balmaz, T.S. Ratiu, Multisymplectic variational integrator for nonsmooth Lagrangian mechanics, in: Forum of Mathematics, Sigma, vol. 4, 2016, http://dx.doi.org/10.1017/fms.2016.17. e19, p. 54.
[22] A.P. Veselov, Integrable discrete-time systems and difference operators, Funkts. Anal. Prilozhen. 22 (1988) 1–13.
[23] J. Moser, A.P. Veselov, Discrete versions of some classical integrable systems and factorization of matrix polynomials, Comput. Math. Phys. 139 (1991) 217–243.
[24] A.P. Veselov, Integrable Lagrangian correspondences and the factorization of matrix polynomials, Funkts. Anal. Prilozhen. 25 (1991) 38–49.
[25] C. Kane, J.E. Marsden, M. Ortiz, Symplectic-energy–momentum preserving variational integrators, J. Math. Phys. 40 (1999) 3353–3371.
[26] J.E. Marsden, S. Pekarsky, S. Shkoller, Discrete Euler-Poincaré and Lie-Poisson equations, Nonlinearity 12 (6) (1999) 1647–1662.
[27] J.E. Marsden, M. West, Discrete mechanics and variational integrators, Acta Numer. 10 (2001) 357–514.
[28] E. Hairer, C. Lubich, G. Wanner, Geometric Numerical Integration: Structure-Preserving Algorithms for Ordinary Differential Equations, in: Springer Series in Computational Mathematics, vol. 31, 2006.
[29] Lily Kharevych, Weiwei, Yiying Tong, Eva Kanso, Jerrold E. Marsden, Peter Schröder, Mathieu Desbrun, Geometric, variational integrators for computer animation, in: ACM/EG Symposium on Computer Animation, 2006, pp. 43–51.
[30] M. Kobilarov, J.E. Marsden, Discrete geometric optimal control on Lie groups, IEE Trans. Robot. 27 (2011) 641–655.
[31] J.E. Marsden, G.W. Patrick, S. Shkoller, Mulltisymplectic geometry, variational integrators and nonlinear PDEs, Comm. Math. Phys. 199 (1998) 351–395.
[32] F. Demoures, F. Gay-Balmaz, M. Kobilarov, T.S. Ratiu, Multisymplectic Lie algebra variational integrator for a geometrically exact beam in $\mathbb{R}^3$, Commun. Nonlinear Sci. Numer. Simul. 19 (10) (2014) 3492–3512. http://dx.doi.org/10.1016/j.cnsns.2014.02.032.
[33] D. Pavlov, P. Mullen, Y. Tong, E. Kanso, J.E. Marsden, M. Desbrun, Structure-preserving discretization of incompressible fluids, Physica D 240 (6) (2011) 443–458.
[34] E. Gawlik, P. Mullen, D. Pavlov, J.E. Marsden, M. Desbrun, Geometric, variational discretization of continuum theories, Physica D 240 (21) (2011) 1724–1760.
[35] M. Desbrun, E. Gawlik, F. Gay-Balmaz, V. Zeitlin, Variational discretization for rotating stratified fluids, Discrete Contin. Dyn. Syst. Ser. A 34 (2) (2014) 479–511.
[36] R.C. Fetecau, J.E. Marsden, M. West, Variational multisymplectic formulations of nonsmooth continuum mechanics, in: Perspectives and Problems in Nonlinear Science, Springer, New York, 2003, pp. 229–261.
[37] R.T. Rockafellar, R.J.-B. Wets, Variational Analysis, in: Grundlehren der Mathematischen Wissenschaften, vol. 317, Springer-Verlag, 1997.
[38] T.J.R. Hughes, R.L. Taylor, J.L. Sackman, A. Curnier, W. Kanoknukulchai, A finite element method for a class of contact-impact problems, Comput. Methods Appl. Mech. Engrg. 8 (1975) 249–276.
[39] R.L. Taylor, P. Papadopoulos, On a finite element method for dynamic contact/impact problems, Internat. J. Numer. Methods Engrg. 36 (1993) 2123–2140.
[40] J.C. Simo, A finite strain beam formulation. The three-dimensional dynamic problem. Part I, Comput. Methods Appl. Mech. Engrg. 49 (1985) 55–70.
[41] F.H. Clarke, Optimization and Nonsmooth Analysis, Wiley, New York, 1983.
[42] J.-J. Moreau, Unilateral contact and dry friction in finite freedom dynamics, in: Nonsmooth Mechanics and Applications, in: J.-J. Moreau, P.D. Panagiotopoulos (Eds.), CISM Courses and Lectures, vol. 302, Springer-Verlag, Vienna, 1988, pp. 1–82.
[43] R.T. Rockafellar, Lagrange multipliers and optimality, SIAM Rev. 35 (2) (1993) 183–238.
[44] R.C. Fetecau, J.E. Marsden, M. Ortiz, M. West, Nonsmooth Lagrangian mechanics and variational collision integrators, SIAM J. Appl. Dyn. Syst. 2 (2003) 381–416.
[45] P. Papadopoulos, R.L. Taylor, A mixed formulation for the finite element solution of contact problems, Comput. Methods Appl. Mech. Engrg. 94 (1992) 373–389.
[46] D. Ellis, F. Gay-Balmaz, D.D. Holm, V. Putkaradze, T.S. Ratiu, Symmetry reduced dynamics of charged molecular strands, Arch. Ration. Mech. Anal. 197 (2) (2010) 811–902.
[47] J.C. Simo, L. Vu-Quoc, A three-dimensional finite-strain rod model. Part II : computational aspects, Comput. Methods Appl. Mech. Engrg. 58 (1986) 55–70.
[48] A. Iserles, H.Z. Munthe-Kaas, S.P. Nørsett, A. Zanna, Lie-group methods, Acta Numer. 9 (2000) 215–365.
[49] N. Bou-Rabee, J.E. Marsden, Hamilton-pontryagin integrators on Lie groups Part I: Introduction and structure-preserving properties, Found. Comput. Math. 9 (2009) 197–219.